IDŐJÁRÁS

QUARTERLY JOURNAL
OF THE HUNGARIAN METEOROLOGICAL SERVICE

CONTENTS

****

http://www.met.hu/Journal-Idojaras.php

VOL. 111 * NO. 4 * OCTOBER – DECEMBER 2007

IDŐJÁRÁS

Quarterly Journal of the Hungarian Meteorological Service

Editorial Office: P.O. Box 39, H-1675 Budapest, Hungary or
Gilice tér 39, H-1181 Budapest, Hungary
E-mail: bozo.l@met.hu or *antal.e@met.hu*
Fax: (36-1) 346-4809

Subscription by

mail: IDŐJÁRÁS, P.O. Box 39, H-1675 Budapest, Hungary;
E-mail: bozo.l@met.hu or *antal.e@met.hu*; *Fax: (36-1) 346-4809*

IDŐJÁRÁS

Quarterly Journal of the Hungarian Meteorological Service
Vol. 111, No. 4, October–December 2007, pp. 221–237

Sensitivity of severe convective storms to soil hydrophysical characteristics: A case study for April 18, 2005

Ákos Horváth[1*], **Ferenc Ács**[2] and **István Geresdi**[3]

[1]*Hungarian Meteorological Service,*
Vitorlás u. 17, H-8600 Siófok, Hungary; E-mail: horvath.a@met.hu

[2]*Department of Meteorology, Eötvös Loránd University,*
P.O. Box 32, H-1518 Budapest, Hungary, E-mail: acs@elte.hu

[3]*University of Pécs, Institute of Environmental Science,*
Ifjúság útja 6, H-7624 Pécs, Hungary; E-mail: geresdi@gamma.ttk.pte.hu

(Manuscript received in final form October 30, 2006)

Abstract—The effect of soil hydraulic properties on formation of severe thunderstorms was investigated by a mesoscale numerical model (Penn State – NCAR MM5). A comparative case study was made to analyze, how two different sets of soil hydrophysical properties, which refer to the same soil texture, affect the convective available potential energy (CAPE), updraft velocity, and precipitation field.

It was found that MM5 simulates adequately the formation and development of severe convective storms. Results of the numerical experiments also show that application of the Hungarian soil hydraulic properties results in formation of more intensive thunderstorm with shorter lifetime than the application of the soil hydraulic properties of the USA. It is shown that application of these site specific soil parameters is important, especially for correct simulation of processes at the meso-γ scale (2–20 km). Further tests are needed to quantify and understand the interrelationships between soil processes and storm events.

Key-words: severe convective storms, soil hydrophysical properties, MM5, Hungary

1. Introduction

Convection refers primarily to atmospheric motions in the vertical direction. The fuel for rising air parcel is the heat energy contained in it. This heat energy can be derived from Earth's surface as sensible heat and from the release of latent heat of condensation and latent heat of fusion. Rising bubbles of hot air, often

* Corresponding author

called thermals, form cumulus clouds in a relatively stable air mass. Rising of thermals in an unstable atmosphere form thunderstorms, which produce heavy rain and hail accompanied by lightning, thunder, and gusty winds. Recently, much more attention is paid to these atmospheric phenomena also in Hungary, because of the caused floods (*Horváth*, 2005a) and wind damages (*Horváth*, 2004, 2005b).

Thunderstorms and convective rainfall are investigated by radar observation (e.g., *Bringi et al.*, 1986; *Höller et al.*, 1994), radiosonde networks (e.g., *Findell* and *Eltahir*, 2003a, 2003b), surface observations (e.g., *Eltahir* and *Pal*, 1996), instrumented airplanes (e.g., *Sinkevich* and *Lawson*, 2005; *Lawson* and *Cooper*, 1990), and by using numerical models (e.g., *Schär et al.*, 1999; *Chen* and *Dudhia*, 2001).

The processes result in formation of severe convective storms are affected by characteristics of both the atmosphere and the land surface. The atmospheric influence is significant via triggering, instability, and interaction between the cloud and environmental air. Storms and precipitation can be triggered by both the upper air disturbances (e.g., *Benjamin* and *Carlson*, 1986; *Lanicci et al.*, 1987; *Findell* and *Eltahir*, 2003c) and the boundary wind convergence (e.g., *Pielke et al.*, 1991a, 1991b; *Avissar* and *Liu*, 1996). Effect on entrainment upon convection and convective precipitation has been analyzed in many aspects (e.g., *Clarke*, 1990; *Betts*, 1992; *Betts et al.*, 1994). The effect of atmosphere near to the surface on convection and convective precipitation has also been studied. Importance of correct calculation of equivalent potential temperature near to the surface was proved by *Eltahir* and *Pal* (1996), *Crook* (1996), *Früh* and *Wirth* (2002). Numbers of papers have been published also about land-surface effects on cloud formation. *Pielke* (2001) discussed and showed the sensitivity of cumulus convective rainfall to the land-surface energy and moisture budgets. The energy and moisture budgets of land-surface are determined by both the land use and the hydraulic properties of soil-vegetation system. The effect of land use and landscape heterogeneity upon cumulus convection was studied by *Segal et al.* (1989), *Rabin et al.* (1990), *Chang* and *Wetzel* (1991), *Li* and *Avissar* (1994), *Chen* and *Avissar* (1994a). The relationship between the Bowen ratio and the deep cumulus convection was discussed by *Segal et al.* (1995). Similar discussions but focusing on the available moisture in the soil-vegetation system is presented by *Segal et al.* (1989), *Chen* and *Avissar* (1994b), *Grasso* (2000), *Pan et al.* (1996).

The purpose of this study is to analyze the sensitivity of convective storms to hydraulic properties of soil-vegetation system. Hydraulic properties of soil-vegetation system are affected by soil hydrophysical properties (*Ács*, 2005). Soil hydrophysical properties depend strongly upon soil texture (*Clapp* and *Hornberger*, 1978; *van Genuchten*, 1980). In meteorological applications, it is assumed that soil texture does not depend upon geographical location (e.g.,

Mölders, 1999; *Mölders* and *Rühaak*, 2002; *Schädler*, 1990). Nevertheless, this assumption is doubted by the number of researchers. Note that *Hodnett* and *Tomasella* (2002) showed, that there is remarkable difference between the characteristics of the same soil texture in the case of temperate and that of tropical soils. The purpose of this study is to prove the sensitivity of formation of convective clouds on soil characteristics by a comparative analysis. In the case study, a convective storm event occurred on April 18, 2005, in the north-eastern part of Hungary (in the vicinity of the settlement Tiszaroff) was investigated. Simulations were made by using both the USA and Hungarian soil data by the Penn State – NCAR MM5 modeling system (fifth-generation meso-scale model). The results obtained are also compared to the surface accumulated precipitation data.

2. *Model description*

2.1. General characteristics of the MM5 model system

The numerical simulations were made by Version 3 of the MM5 (NCAR-PSU Mesoscale Model) (*Dudhia*, 1993). In the model, a terrain-following sigma coordinate system is applied. The predictive variables are: pressure perturbation, the three momentum components, temperature, specific humidity, and the mixing ratio of the different type of hydrometeors (cloud water, cloud ice, rain, snow, and graupel particles). For this study, the model is integrated with horizontal resolutions of 6 km, and with 26 vertical levels. The partial differential equations system is solved by using a relaxation lateral boundary condition and a radiation upper boundary condition.

2.2. Convection and cloud physics parameterization

Grell's scheme (*Grell et al.*, 1994) is applied for parameterization of convection based on rate of destabilization or quasi-equilibrium, simple single-cloud scheme with updraft and downdraft fluxes and compensating motion determining heating/moistening profile. Explicit bulk microphysical scheme with five different types of hydrometeors was used to simulate the formation of cloud and precipitation elements (*Reisner et al.*, 1998). The hydrometeors are: cloud water, cloud ice, rain, snow, and graupel particles. Collision coalescence process between different type of hydrometeors, furthermore, diffusion of vapor, freezing of liquid elements, and melting of ice particles were simulated. Equation of conservation was not only solved for the mixing ratios of hydrometeors but for the number concentration of cloud ice as well.

2.3. *PBL scheme and land-surface model*

The planetary boundary layer (PBL) is described by the non-local PBL scheme based on *Troen* and *Mahrt* (1986). Compared with other non-local or high-order closure schemes, this PBL scheme proved to be more efficient, because it needs less computer capacity. Land-surface processes are simulated by OSU LSM (Oregon State University Land-surface Model). It is based on the coupling of Penman's potential evaporation approach (*Penman*, 1948) modified by atmospheric stratification effect (*Mahrt* and *Ek*, 1984), the multi-layer soil model (*Mahrt* and *Pan*, 1984), and the single-layer canopy model (*Pan* and *Mahrt*, 1987). Actual evapotranspiration is simulated by using the so-called β-approach based on the moisture availability concept: β depends upon both the land-surface and the atmospheric characteristics (see Eqs. (15) and (13) in papers of *Chen* and *Dudhia* (2001) and *Chen et al.* (1996), respectively). Canopy resistance is formulated after *Jarvis* (1976) using relative stomatal conductivity formulae of *Noilhan* and *Planton* (1989). Atmospheric stratification is simulated by applying the Monin-Obukhov similarity theory (*Oncley* and *Dudhia*, 1995). Recently, as in our simulations too, surface exchange coefficients for heat and moisture are given by using lookup tables. Surface skin temperature (T_{skin}) of combined vegetation-ground layer is calculated by a linearized surface energy balance equation (see, for instance, Eq. (4) of *Sridhar et al.*, 2002). This simple equation has to be solved by numeric iteration technique for the implicit relationships between T_{skin} and surface energy balance components. Soil moisture and temperature are calculated by Richards' and heat flow equations, respectively. A more extensive description of these processes can be found, for instance, in papers of *Chen* and *Dudhia* (2001) and *Sridhar et al.* (2002).

3. *Data and numerical experiments*

3.1. *The synoptic situation*

Initial condition fields applied for numerical experiments are obtained from the ECMWF analysis and surface and upper air observations. ECMWF analysis of basic state variables (temperature, humidity, wind, geodynamical height) on mandatory levels up to 100 hPa at 12:00 UTC on April 18, 2005 are considered as first guess data. Surface synoptic information and some sounding data are smoothed to the first guess using Cressman scheme. Boundary conditions are given by the ECMWF forecasts. According to data, the initial surface (1st soil layer) soil moisture field can be characterized as relatively dry.

The weather of the investigated day was determined by a slowly moving cyclone with center situated above the eastern part of the Carpathian Basin. In

lower layers of the cyclone (850 hPa) moist and warm air mass was drifted above the basin, meanwhile on higher levels (500 hPa) cold advection occurred, causing convective instability. During afternoon several thunderstorms were formed, and some of them caused flash floods in the mountains of the north-eastern regions of Hungary. During the day many convective storms were also observed over the plane regions. Detailed description of the synoptic situation is presented by *Horváth* (2005a).

Because the storms were formed both over flat and mountainous regions, this case offers a good opportunity to investigate how the soil hydrophysical characteristics affect the cloud formation at different geographical conditions.

3.2. Land-surface characteristics and parameter specification

The region, where the formation and development of the thunderstorms was investigated, is a relatively flat area along the river Tisza. According to the MM5 dataset, the vegetation characteristics in this region for April are as follows: The vegetation type is "cultivations", the green vegetation fraction is 0.6–0.7, the minimal stomatal resistance is 40 s m^{-1}, the albedo is 0.19, the roughness length is 0.075 m. The leaf area index (LAI) is prescribed, but the vegetation fraction is estimated on the basis of NDVI (Normalized Difference Vegetation Index). Details concerning the specification of vegetation parameters are described in the work of *Chen* and *Dudhia* (2001).

According to the soil data set of the MM5 model, clay loam is the prevailing soil texture in the region investigated. It has to be noted that there are also sandy loam patches here. Soil hydrophysical properties (saturated soil moisture content θ_S, saturated soil water retention Ψ_S, saturated water conductivity K_S, pore size distribution index b, field capacity soil moisture content θ_f, and wilting point soil moisture content θ_w) referring to all 12 soil textures are given in *Table 1*. Of course, these parameters refer to the soil characteristics of the USA. The same parameters were determined for Hungarian soils using the works of *Nemes* (2003) and *Fodor* and *Rajkai* (2005). The corresponding soil hydrophysical properties are presented in *Table 2*.

It is obvious that there are remarkable differences between the USA and Hungarian parameters. Let us take a look to the values of pore size distribution index b. For finer soil textures in the USA, b values are larger than the corresponding Hungarian b values. Clay loam soil texture is of interest to us. pF-curves ($\log|\Psi(\text{cm } H_2O)|$ as the function of relative/scaled soil moisture content) and soil water conductivity functions for the USA and Hungarian clay loam are presented in *Fig. 1*. The figure shows, that there are large differences between the USA and Hungarian $K(\Psi)$ functions. The Hungarian $K(\Psi)$ is about 2 orders of magnitude larger than the USA $K(\Psi)$, independently of the value of Ψ (*Fig. 1b*).

Table 1. USA soil parameters used in the MM5 model. Symbols: θ_S = saturated soil moisture content, Ψ_S = saturated soil water retention, K_S = saturated water conductivity, b = pore size distribution index, θ_f = field capacity soil moisture content, and θ_w = wilting point soil moisture content

Soil texture	θ_S ($m^3\ m^{-3}$)	Ψ_S (m)	K_S ($m\ s^{-1}$)	b	θ_f ($m^3\ m^{-3}$)	θ_w ($m^3\ m^{-3}$)
Sand	0.339	0.069	$4.60 \cdot 10^{-5}$	2.79	0.236	0.010
Loamy sand	0.421	0.036	$1.41 \cdot 10^{-5}$	4.26	0.283	0.028
Sandy loam	0.434	0.141	$5.23 \cdot 10^{-6}$	4.74	0.312	0.047
Silt loam	0.476	0.759	$2.81 \cdot 10^{-6}$	5.33	0.360	0.084
Silt	0.476	0.759	$2.81 \cdot 10^{-6}$	5.33	0.360	0.084
Loam	0.439	0.355	$3.38 \cdot 10^{-6}$	5.25	0.329	0.066
Sandy clay loam	0.404	0.135	$4.45 \cdot 10^{-6}$	6.66	0.314	0.067
Silty clay loam	0.464	0.617	$2.04 \cdot 10^{-6}$	8.72	0.387	0.120
Clay loam	0.465	0.263	$2.45 \cdot 10^{-6}$	8.17	0.382	0.103
Sandy clay	0.406	0.098	$7.22 \cdot 10^{-6}$	10.73	0.338	0.100
Silty clay	0.468	0.324	$1.34 \cdot 10^{-6}$	10.39	0.404	0.126
Clay	0.468	0.468	$9.74 \cdot 10^{-7}$	11.55	0.412	0.138

Table 2. Hungarian soil parameters used in the MM5 model. Symbols: θ_S = saturated soil moisture content, Ψ_S = saturated soil water retention, K_S = saturated water conductivity, b = pore size distribution index, θ_f = field capacity soil moisture content, and θ_w = wilting point soil moisture content

Soil texture	θ_S ($m^3\ m^{-3}$)	Ψ_S (m)	K_S ($m\ s^{-1}$)	b	θ_f ($m^3\ m^{-3}$)	θ_w ($m^3\ m^{-3}$)
Sand	0.409	0.420	$3.26 \cdot 10^{-5}$	1.14	0.189	0.001
Loamy sand	0.414	0.450	$2.52 \cdot 10^{-5}$	2.43	0.233	0.017
Sandy loam	0.425	0.610	$1.14 \cdot 10^{-5}$	3.97	0.283	0.099
Silt loam	0.458	1.010	$2.73 \cdot 10^{-6}$	4.33	0.333	0.068
Silt	0.464	3.190	$2.00 \cdot 10^{-6}$	3.54	0.328	0.072
Loam	0.424	1.530	$4.58 \cdot 10^{-6}$	4.06	0.296	0.064
Sandy clay loam	0.430	0.340	$7.98 \cdot 10^{-6}$	5.18	0.311	0.063
Silty clay loam	0.436	5.680	$6.20 \cdot 10^{-7}$	4.18	0.338	0.093
Clay loam	0.430	4.170	$3.05 \cdot 10^{-6}$	4.05	0.306	0.083
Sandy clay	0.500	0.890	$4.58 \cdot 10^{-6}$	3.58	0.340	0.055
Silty clay	0.453	11.760	$1.05 \cdot 10^{-6}$	4.06	0.340	0.113
Clay	0.499	14.930	$8.00 \cdot 10^{-7}$	3.97	0.378	0.130

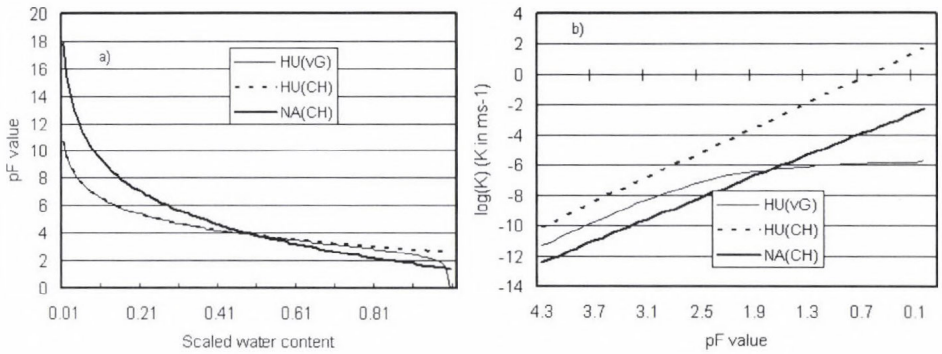

Fig. 1. Soil water retention (given as pF value) as a function of scaled water content (a), and soil water conductivity curves of clay loam for the USA and Hungarian soil data (b). Symbols: HU(vG) = Hungarian soil data, *van Genuchten*'s (1980) parameterization, HU(CH) = Hungarian soil data, *Clapp* and *Hornberger*'s (1978) parameterization, and NA(CH) = USA soil data, *Clapp* and *Hornberger*'s (1978) parameterization.

3.3. Numerical experiments

Since the differences between the USA and Hungarian soil parameters are rather large, numerical experiments are performed for both the USA and Hungarian soil parameters. Although some observations show that the soil texture applied in the MM5 data set is not appropriate for use in Hungary, only soil hydrophysical parameters were changed, the area distribution of soil texture was not modified. In the following, results obtained using USA soil parameters will be briefly referred to as US results, and results obtained using Hungarian soil parameters will be briefly referred to as HU results.

4. Validation, comparison, and discussion

4.1. Validation of the simulated 24 hours precipitation fields

Predicted field of the 24 hours accumulated precipitation is presented in *Fig. 2b*. The calculated data agree well with observations, which were created from rain gauge network 06:00 UTC observations on April 19, 2005 (*Fig. 2a*). Thunderstorms moved from northeast to southwest left significant "tracks". Most of the precipitation measured on the eastern part of Hungary fell between 12:00 and 18:00 UTC on April 18 allowing comparison of modeled and observed precipitation data. The precipitation track starting from the north-eastern part of Hungary can be well identified on the simulated field (*Fig. 2b*). A weaker precipitation field (denoted by P3 in *Fig.* 2b) in the southeast region of Hungary can be identified as part of a south-eastern track. The north-eastern

precipitation system (denoted by P1 in *Fig. 2b*) was forced by mountains, therefore, it was much heavier than the thunderstorms in the south-eastern track (denoted by P3 in *Fig. 2b*). In the middle of the track, near to the region of the Tisza Lake, thunderstorms were formed and moved over the flat areas of the Great Hungarian Plain (denoted by P2 in *Fig. 2b*). In this region, the influence of soil hydrophysical properties upon the evolution of thunderstorms is not suppressed by mountains forced convection. Note that MM5 reproduced not only the formation and development of thunderstorms on the Great Hungarian Plain, but also the flash flood event (*Horváth*, 2005a) in the mountainous area (denoted by P4 in *Fig. 2b*).

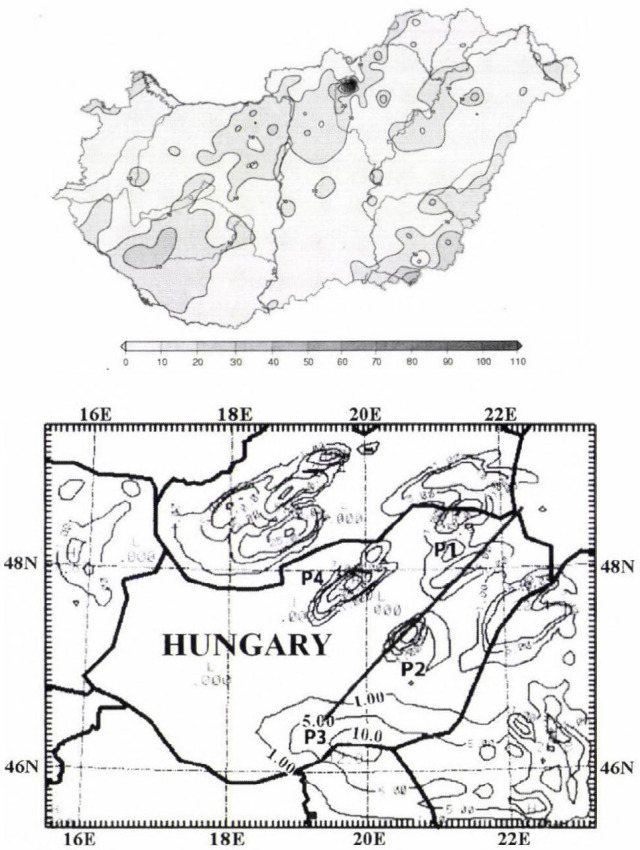

Fig. 2. Observed 24 hours cumulated precipitation measured at 06:00 UTC on April 19, 2005 (up), and the same field simulated by the MM5 model (down). The straight line indicates the position of the vertical cross section displayed in *Fig. 7*. The symbols P1, P2, P3, and P4 denote different precipitation systems. On the east of the river Danube, the precipitation fell mostly between 12:00 and 18:00 UTC of April 18. The calculation was made by using the USA soil data.

4.2. Comparison of surface available energy fields

The surface available energy, A_e (latent plus sensible heat flux) is an important forcing factor in evolution of thunderstorms. It affects their intensity and dynamics. Areal distribution of A_e at 18:00 UTC for the US and HU cases is shown in *Fig. 3*. While in the HU case A_e is generally negative (about from –10 to –50 W m^{-2}), in the US case positive A_e values (up to 50 W m^{-2}) are prevailing. This difference can explain why new convective clouds are formed in the US case at 18:00 UTC, and why the thunderstorms start to be dissipated in the HU case at the same time. These results show that thunderstorm dynamics in the US and HU cases are rather different.

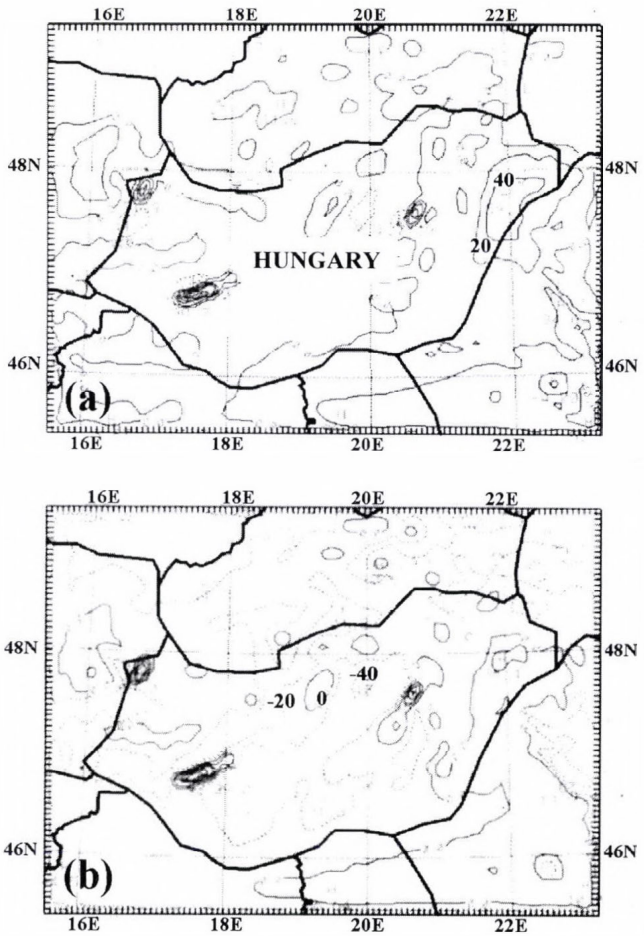

Fig. 3. Computed surface available energy fields obtained by the MM5 modeling system using the USA (a) and Hungarian (b) soil parameters at 18:00 UTC.

4.3. Comparison of convective available potential energy fields

The fields of convective available potential energy (CAPE) are analyzed to investigate the convective energy of thunderstorm. *Fig. 4* shows that there are no significant differences between the US and HU CAPE fields at the beginning of the integration time (15:00 UTC). In both cases, larger CAPE values (the highest values are between 500–700 Jkg^{-1}) could be found in the eastern part of Hungary (close to the river Tisza), than in the mountainous region of north Hungary. This shows that the development of thunderstorms above the walley of the river Tisza was more affected by the value of CAPE than above the mountainous region, where the presence of hills contributes to the formation of intensive thunderstorms.

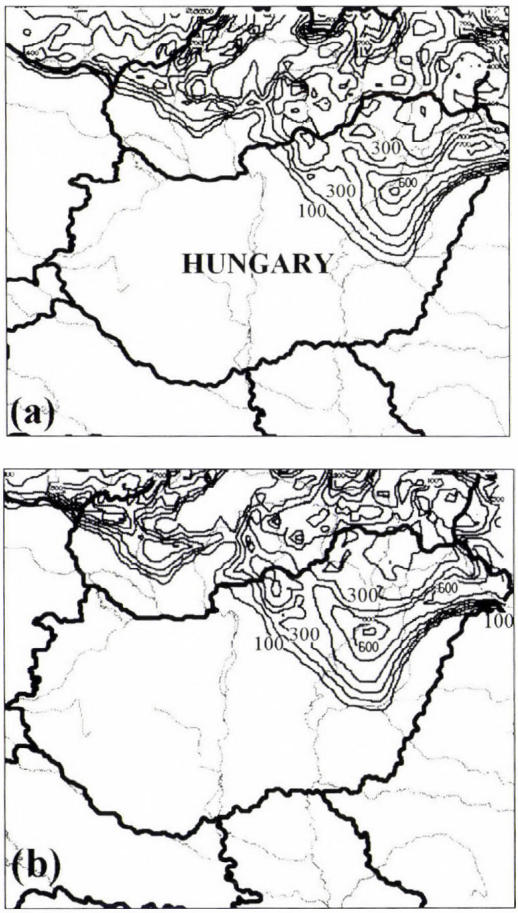

Fig. 4. Calculated convective available potential energy fields obtained by using the USA (up) and Hungarian (down) soil parameters at 15:00 UTC.

Although the difference between the CAPE fields of the HU and US cases was negligible at the beginning of the calculation, by the end of the integration, differences between the US and HU CAPE fields becomes more significant. While in the HU case the energy has already been used up by thunderstorms (*Fig. 5b*) by the end of the simulation, in the US case high CAPE values of 500 J kg^{-1} (*Fig. 5a*) could be observed over a large region. This also unequivocally shows, that the thunderstorms in the HU case are more intensive and developing faster than the ones in the US case.

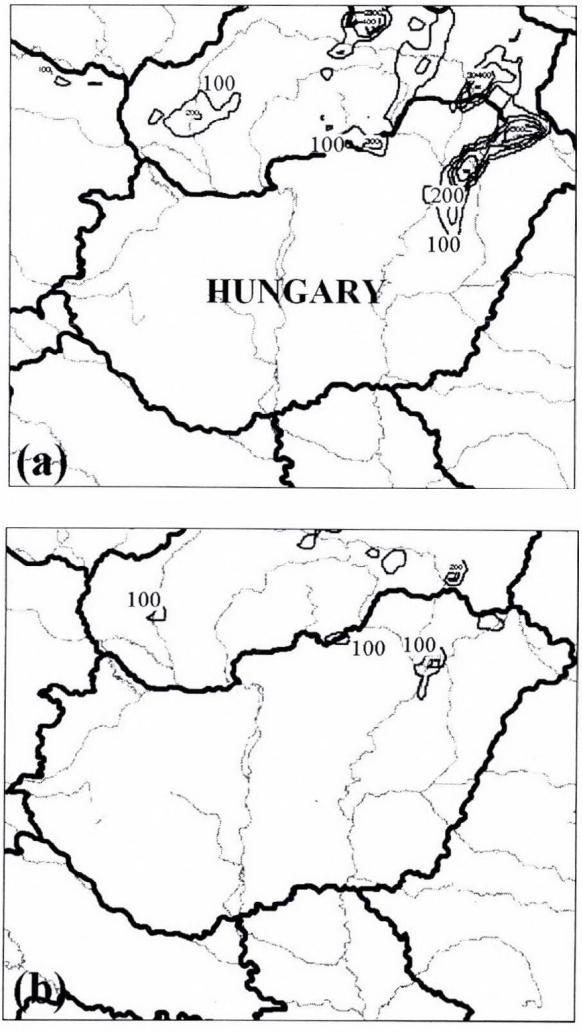

Fig. 5. As in *Fig. 4*, but at 18:00 UTC.

4.4. *Comparison of vertical velocity fields at 925 hPa height*

The transfer of heat and vapor between the surface and the convective clouds occurs in the planetary boundary layer (PBL). One of its important characteristics is the vertical velocity (*w)* at the level of 925 hPa (about 100 m above the surface level). *Fig. 6* shows the vertical velocity fields (*w*) values for both the US and HU cases at 17:00 UTC. While negative values mean descending motion, positive values represent ascending motion. In the US case, the boundary line between the ascending and descending regions is going from northwest to southeast. In spite of this, in the HU case the same boundary line is going from southwest to northeast. The thunderstorm in the HU case is much closer to Tiszaroff, than the thunderstorm in the US case. While this difference is remarkably considerable at meso-γ scale (2–20 km) (see *Orlanski*, 1975), it is negligible at meso-β scale.

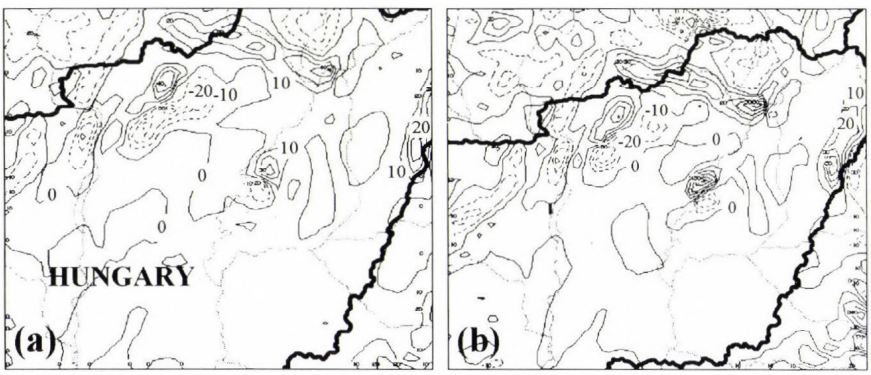

Fig. 6. Vertical velocity fields at the 925 hPa level obtained by using the USA (a) and Hungarian (b) soil parameters at 17:00 UTC. The continuous and dashed lines mean upward and downward direction, respectively. The vertical velocity components are given in cm s^{-1}.

4.5. *Comparison of vertical velocities in clouds*

Two dimensional representation of vertical velocities in clouds (w_{CL}) along the line presented in *Fig. 2b* at 16:00 UTC for both US and HU cases is shown in *Fig. 7*. Two updraft regions could be recognized. The first region, going from southwest to northeast is in the vicinity of Tiszaroff. The second one is close to Tiszalök. The first region seems to be more intensive comparing to the second one. The largest velocity is about 4 m s^{-1}. (It has to be noted, that the updraft velocity in the real thunderstorm must have been about 10 m s^{-1} in about a few km wide region. The much smaller calculated updraft velocity is the consequence of the crude horizontal resolution of 6 km.) While in the US case, the region where the updraft velocity is larger than 4 m s^{-1} is located in a shallow layer

between 600–560 hPa, in the HU case the same region is in a deeper layer between 700–480 hPa. It is also obvious, that the thunderstorm close to Tiszaroff is deeper and more intensive in the HU case than in the US case.

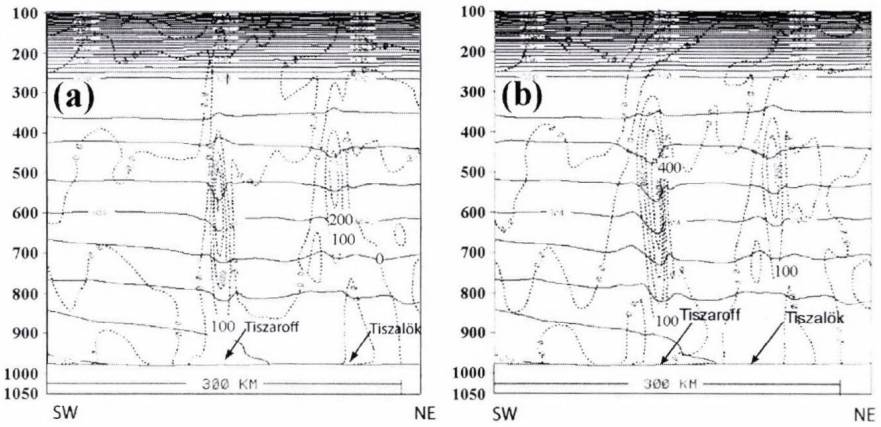

Fig. 7. Simulated vertical velocity fields along the line indicated in *Fig. 2b* using the USA (a) and Hungarian (b) soil parameters at 16:00 UTC. The positions of the settlements mentioned in the text are denoted in the figures. The direction of the cross-section is also shown. Dotted lines denote the isolines for vertical velocity component in cm s^{-1}. Solid lines denote the potential temperature.

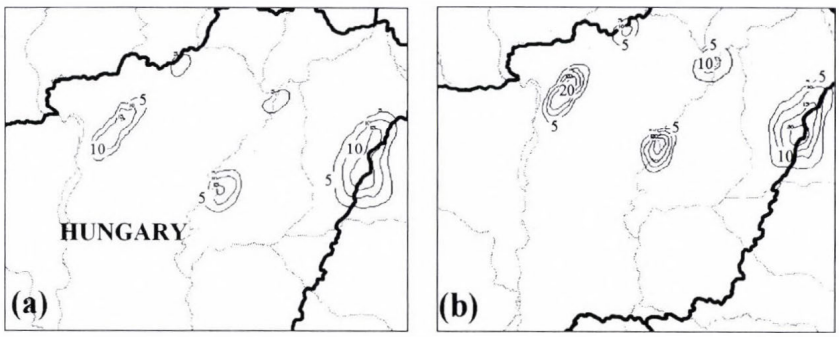

Fig. 8. 15 minutes cumulated precipitation fields obtained by the MM5 modeling system at 18:00 UTC using the USA (a) and Hungarian (b) soil parameters.

4.6. Comparison of precipitation fields at 18:00 UTC

The change of the soil hydrophysical characteristics also affects the precipitation field. Simulated fields of 15 minutes accumulated precipitation at 18:00 UTC for the US and HU case are presented in *Fig. 8*. It is noticeable, that precipitation is somewhat more intensive for the HU than for the US case. This is valid not only for the region close to Tiszaroff but also for the region close to Tiszalök.

5. *Conclusions*

In this study, the impact of soil hydrophysical properties upon the formation and development of severe convective storms is investigated. Analysis is performed modeling a convective storm event on April 18, 2005, in the vicinity of the settlement Tiszaroff. The Penn State – NCAR MM5 modeling system was used to make the numerical simulation. The calculation was made by both USA and Hungarian soil data. The sensitivity of the formation and development of the thunderstorms to soil hydrophysical characteristics was investigated by comparison of the results of the US and HU runs. The simulation results were also compared with observations. The results obtained can be summarized as follows:

- The MM5 is an appropriate tool for modeling severe convective storms. Simulated precipitation fields agree well with observations in meso-β scale. Unfortunately, no observation database is available to make the comparison in meso-γ scale.
- The parameters (CAPE, w at 925 hPa level, w_{CL}, and precipitation field) characterizing the thunderstorms are sensitive to changes of soil hydrophysical properties (Ψ_S, K_S, b, θ_S, θ_f, θ_w). Differences are particularly obvious in meso-γ scale.
- Both the intensivity and life time of the thunderstorms depends on the soil hydrophysical properties. Application of Hungarian soil characteristics results in formation of deeper thunderstorms with shorter life time. This difference in the dynamics could be related to the different amount of the accumulated precipitation. In the case of the HU run, the calculated accumulated precipitation was significantly larger than that of in the case of the US run. Due to absence of the data in meso-γ scale, we were not able to verify this difference.

Obviously, further tests are needed. For example, we should have to prove that it is more favorable to use site specific soil parameters than anything else (in this case USA parameters are taken), not only for modeling of land surface processes but also for modeling of severe convective storms. This validation experiment is a task for future.

Acknowledgements—This study is financially supported by the Hungarian Scientific Research Fund OTKA, project number T043010 and by the National Program for Research and Development (project number NKFP3-00022/2005). We thank *Mrs. Hajnalka Breuer* for helping in construction of the figures.

References

Avissar, R. and *Liu, Y.*, 1996: Three-dimensional numerical study of shallow convective clouds and precipitation induced by land surface forcing. *J. Geophys. Res. 101*, 7499-7518.

Ács, F., 2005: On transpiration and soil moisture contentsensitivity to soil hydrophysical data. *Bound.-Lay. Meteorol. 115*, 473-497.

Benjamin, S.G. and *Carlson, T.N.*, 1986: Some effects of surface heating and topography ont he regional severe storm environment, I. Three-dimensional simulations. *Mon. Wea. Rev. 114*, 307-329.

Betts, A.K., 1992: FIFE atmospheric boundary layer budget methods. *J. Geophys. Res. 97*, 18523-18531.

Betts, A.K., Ball, J.H., Beljaars, A.C.M., Miller, M.J., and *Viterbo, P.*, 1994: Coupling between land-surface boundary-layer parameterizations and rainfall on local and regional scales. Lessons from the wet summer of 1993. *Fifth Conference on Global Change Studies*. Am. Meteorol. Soc., Boston, 174-181.

Bringi, V.N., Rasmussen, R.M., and *Vivekanandan, J.*, 1986: Multiparameter radar measurements in Colorado convective storms. Part I: Graupel melting studies. *J. Atmos. Sci. 43*, 2545-2562.

Chang, J.T. and *Wetzel, P.J.*, 1991: Effects of spatial variations of soil moisture and vegetation ont he evolution of a prestorm environment: A case study. *Mon. Weather Rev. 119*, 1368-1390.

Chen, F. and *Avissar, R.*, 1994a: The impact of land-surface wetness heterogeneity on mesoscale heat fluxes. *J. Appl. Meteorol. 33*, 1323-1340.

Chen, F. and *Avissar, R.*, 1994b: Impact of land-surface moisture variabilities on local shallow convective cumulus and precipitation in large-scale models. *J. Appl. Meteorol. 33*, 1382-1394.

Chen, F. and *Dudhia, J.*, 2001: Coupling and Advanced Land Surface-Hydrology Model with the Penn State-NCAR MM5 Modeling System. Part I. Model Implementation and Sensitivity. *Mon. Weather Rev. 129*, 569-585.

Chen, F., Mitchell, K., Schaake, J., Xue, Y., Pan, H.L., Koren, V., Duan, Q.Y., Ek, M., and *Betts, A.*, 1996: Modeling of land surface evaporation by four schemes and comparison with FIFE observations. *J. Geophys. Res. 101*, 7251-7268.

Clapp, R.B. and *Hornberger, G.M.*, 1978: Empirical Equations for Some Hydraulic Properties. *Water Resour. Res. 14*, 601-604.

Clarke, R.H., 1990: Modeling mixedlayer growth in the Koorin experiment. *Aust. Meterol. Mag. 38*, 227-234.

Crook, N.A., 1996: Sensitivity of moist convection forced by boundary layer processes to low-level thermodynamic fields. *Mon. Weather Rev. 124*, 1767-1785.

Dudhia, J., 1993: A non-hydrostatic version of the Penn State-NCAR Mesoscale Model: Validation tests and simulation of an Atlantic cyclone and cold front. *Mon. Weather Rev. 121*, 1493 - 1513.

Eltahir, E.A.B., and *Pal, J.S.*, 1996: Relationship between surface conditions and subsequent rainfall in convective storms. *J. Geophys. Res. 101*, 26237-26245.

Findell, K.L. and Eltahir, *E.A.B.*, 2003a: Atmospheric Controls on Soil Moisture-Boundary Layer Interactions. Part I: Framework Developement. *J. Hydrometeorol. 4*, 552-569.

Findell, K.L. and *Eltahir, E.A.B.*, 2003b: Atmospheric Controls on Soil Moisture-Boundary Layer Interactions. Part II: Feedbacks within the Continental United States. *J. Hydrometeorol. 4*, 570-583.

Findell, K.L. and *Eltahir, E.A.B.*, 2003c: Atmospheric controls on soil moisture-boundary layer interactions: Three-dimensional wind effects. *J. Geophys. Res. 108, No. D8*, 8385, doi: 10.1029/2001JD0015152003.

Fodor, N. and *Rajkai, K.*, 2005: Estimation of Physical Soil Properties and Their Use in Models. *Agrokem Talajtan 54*, 25-40.

Früh, B. and *Wirth, V.*, 2002: The role of surface wet-bulb temperature for subsequent convective rainfall in midlatitudes. *Poster presentation at European Geophysical Society, XVII General Assembly*, April 22-26, Nice, France. [Available as pdf-document on http://www.staff.uni-mainz.de/frueh/publics.html]

Grasso, L.D., 2000: The numerical simulation of dryline formation on soil moisture. *Mon. Weather Rev. 128*, 2816-2834.

Grell, G., Dudhia, J., and *Stauffer, D.*, 1994: A description of the fith generation Penn State/NCAR Mesoscale Model. *NCAR Tech. Note NCAR/TN-398+STR*, 117 pp.

Horváth, Á., 2004: The great storm on November 19, 2004 (in Hungarian). *Légkör XLIX,* No. 4, 6-9.

Horváth, Á., 2005a: Meteorological backround of flooding in Mátrakeresztes on April 18, 2005 (in Hungarian). *Légkör 50,* No. 2, 6-9.

Horváth, Á., 2005b: Meteorological description of the storm on May 18, 2005 (in Hungarian). *Légkör 50,* No. 3, 12-16.

Höller, H., Bringi, V.N., Hubbert, J., Hagen, M., and *Meischner, P.F.*, 1994: Life cycle and precipitation formation in a hybrid-type hailstorm revelaed by polarimetric and Doppler radar measurements. *J. Atmos. Sci. 51*, 2500-2522.

Hodnett, M.G. and *Tomasella, J.*, 2002: Marked differences between van Genuchten soil water-retention parameters for temperate and tropical soils: a new water-retention pedo-transfer function developed for tropical soils. *Geoderma 108,* 155-180.

Jarvis, P. G., 1976: The interpretation of the variations in the leaf water potential and stomatal conductance found in canopies in the field. *Philos. T. R. Soc. B. 273*, 593-610.

Lanicci, J.M., Carlson, T.N., and *Warner, T.T.*, 1987: Sensitivity of the great plains severe-storm environment to soil moisture distribution. *Mon. Weather Rev. 115*, 2660-2673.

Lawson, R.P. and *Cooper, W.A.*, 1990: Performance of some airborne thermometers in clouds. *J. Atmos. Ocean. Tech. 7*, 480-494.

Li, B., and *Avissar, R.*, 1994: The impact of spatial variability of land-surface heat fluxes. *J. Clim.* 7, 527-537.

Mahrt, L. and *Ek, M.*, 1984: The Influence of Atmospheric Stability on Potential Evaporation. *J. Clim. Appl. Meteorol. 23*, 222-234.

Mahrt, L. and *Pan, H.L.*, 1984: A two-layer model of soil hydrology. *Bound.-Lay. Meteorol. 29*, 1-20.

Mölders, N., 1999: Einfache und akkumulierte Landnutzungsänderungen und ihre Auswirkungen auf Evapotranspiration, Wolken- und Niederschlagsbildung. *Wissenschaftlichen Mitteilungen aus dem Institut für Meteorologie der Universität und dem Institut für Troposphärenforschung e. V. Leipzig.* BAND 15, ISBN 3-9806117-4-4. [Available at ELTE, Department of Meteorology, Pázmány Péter sétány 1/A., 1117 Budapest]

Mölders, N. and *Rühaak, W.*, 2002: On the impact of explicitly predicted runoff on the simulated atmospheric response to small-scale land-use changes – an integrative modeling approach. *Atmos. Res. 63(1-2)*, 3-38.

Nemes, A., 2003: Multi-scale hydraulic pedotransfer functions for Hungarian soils. *Ph. D. Dissertation. Wageningen Universiteit.* ISBN 90-5808-804-9. 143 p.

Noilhan, J., and *Planton, S.*, 1989: A simple parameterization of land surface processes for meteorological models. *Mon. Weather Rev. 117*, 536-549.

Oncley, S.P. and *Dudhia, J.*, 1995: Evaluation of surface fluxes from MM5 using observations. *Mon. Weathr Rev. 123*, 3344-3357.

Orlanski, I., 1975: A Rational Subdivision of Scales for Atmospheric Processes. *B. Am. Meteorol. Soc. 56*, 527-530.

Pan, H.L. and *Mahrt, L.*, 1987: Interaction between soil hydrology and boundary-layer developement. *Bound.-Lay. Meteorol. 38*, 185-202.

Pan, Z., Takle, E., Segal, M., and *Turner, R.*, 1996: Influences of model parameterization schemes on the response of rainfall to soil moisture in the central United States. *Mon. Weather Rev. 124*, 1786-1802.

Penman, H.L., 1948: Natural evaporation from open water, bare soil and grass. *Proc. R.. Soc. Lond. A193*, 120-195.

Pielke, R.A., 2001: Influence of the spatial distribution of vegetation and soils on the prediction of cumulus convective rainfall. *Rev. Geophys. 39*, 151-177.

Pielke, R.A., Dalu, G., Snook, J.S., Lee, T.J., and *Kittel, T.G.F.*, 1991a: Nonlinear influnce of mesoscale land use on weather and climate. *J. Clim. 4*, 1053-1069.

Pielke, R.A., Song, A., Michaels, P.J., Lyons, W.A., and *Arritt, R.W.*, 1991b: The predictibility of sea-breeze generated thunder-storms. *Atmosfera 4*, 65-78.

Reisner, J., Rasmussen, R. M., and *Bruintjes, R.T.*, 1998: Explicit forecasting of supercooled liquid water in winter storms using the MM5 mesoscale model. *Q. J. Roy. Meteor. Soc. 124*, 1071-1107

Rabin, R.M., Stadler, S., Wetzel, P.J., Stensrud, D.J., and *Gregory, M.*, 1990: Observed effects of landscape variability on convective clouds. *B. Am. Meteorol. Soc. 71*, 272-280.

Schädler, G., 1990: Numerische Simulationen zur Wechselwirkung zwischen Landoberflächen und atmospherischer Grenzschicht. Wissenschaftliche Berichte des Instituts für Meteorologie und Klimaforschung der Universität Karlsruhe. Nr. 13, ISSN 0179-5619. [Available at ELTE, Department of Meteorology, Pázmány Péter sétány 1/A., H-1117 Budapest]

Schär, C., *Lüthi*, *D.*, *Beyerle*, *U.*, and *Heise*, *E.*, 1999: The Soil-Precipitation Feedback: A Process Study with a Regional Climate Model. *J. Climate 12*, 722-741.

Segal, *M.*, *Garratt*, *J.R.*, *Kallos*, *G.*, and *Pielke*, *R.A.*, 1989: The impact of wet soil and canopy temperatures on daytime boundary-layer growth. *J. Atmos. Sci. 46*, 3673-3684.

Segal, *M.*, *Arritt*, *R.W.*, *Clark*, *C.*, *Rabin*, *R.*, and Brown, *J.*, 1995: Scaling evaluation of the effect of surface characteristics on potential for deep convection over uniform terrain. *Mon. Weather Rev. 123*, 383-400.

Sinkevich, *A.A.*, and *Lawson*, *R.P.*, 2005: A Survey of Temperature Measurements in Convective Clouds. *J. Appl. Meteorol. 44*, 1133-1145.

Sridhar, *V.*, *Elliott*, *R.L.*, Chen, *F.*, and *Brotzge*, *J.A.*, 2002: Validation of the NOAH-OSU land surface model using surface flux measurements in Oklahoma. *J. Geophys. Res., 107, NO. D20*, 4418, doi: 10.1029/2001JD001306.

Troen, *I.*, and *Mahrt*, *L.*, 1986: A simple model of the atmospheric boundary layer: Sensitvity to surface evaporation. *Bound.-Lay. Meteorol. 37*, 129-148.

van Genuchten, *M. Th.*, 1980: A Closed-Form Equation for Predicting the Hydraulic Conductivity of Unsaturated Soils. *Soil Sci. Soc. Am. J. 44*, 892-898.

IDŐJÁRÁS

Quarterly Journal of the Hungarian Meteorological Service
Vol. 111, No. 4, October–December 2007, pp. 239–250

Estimation of surface energy and carbon balance components in the vicinity of Debrecen using Thornthwaite's bucket model

Gábor Szász[1], **Ferenc Ács**[2*] and **Hajnalka Breuer**[2]

[1]*Centre of Agricultural Sciences, University of Debrecen, P.O. Box 36, H-4015 Debrecen, Hungary*

[2]*Department of Meteorology, Eötvös Loránd University, P.O. Box 32, H-1518 Budapest, Hungary, E-mail: acs@elte.hu*

(Manuscript received in final form July 12, 2007)

Abstract—Surface energy and carbon balance components are calculated in the vicinity of Debrecen (Hungary) using extended Thornthwaite's bucket model. Soil water content prediction module of the model is tested and verified against measured data of the Agrometeorological Observatory of the University of Debrecen in the period 1972–1992. Energy and carbon balance components estimated are not verified because of the missing direct measurements.

The annual course of components, sensitivity of components to field capacity soil water content changes, and statistical relationships between some energy, water, and carbon balance components are discussed. Among the results it is worth mentioning the sensitive coupling between field capacity water content, actual evapotranspiration, and net ecosystem exchange. Results obtained are useful in describing Debrecen's regional climate.

Key-words: bucket model; energy-, water- and carbon balance; net ecosystem exchange; field capacity, Debrecen

1. Introduction

The Agrometeorological Observatory of the University of Debrecen is an agrometeorological site where a long time series of measured soil water content data is also available. These data combined with long term measurements of relevant meteorological elements, such as global radiation (*Rs*) or sunshine

* Corresponding author

duration, air temperature (T), and precipitation (P) enable us to get an insight into the climatology of energy and carbon balance components of the region.

Debrecen's climate and other environmental characteristics have been analyzed by *Justyák* and *Tar* (1994) using simple data processing. The analysis has been based on measured quantities during the 20th century. A more extensive analysis using different empirical approaches for estimating surface energy balance components was done by *Szász* (2002). In these calculations the quantities were diagnostically estimated using measured soil water content data from the period 1964–1993. Recently, a diagnostic analysis using micro-meteorological methods has been performed by *Ács et al.* (2005). This approach used not only soil water content but also ground surface temperature data. The calculations referred to period 1974–1986. Soil water content data are used for verifying the model. According to the results, there are many limitations in estimating energy balance components.

Monthly mean values of energy balance components can be estimated using the bucket method of *Thornthwaite* (1948), avoiding enormous data processing and all limitations arising from the need to scale up the outputs in time and space. Besides, Thornthwaite's model can be simply extended for estimating actual evapotranspiration and carbon balance components of soil-vegetation system.

On the basis of all these, the aim of this study is to analyze the energy and carbon balance components from climatological point of view. In doing so, we focus on

- verifying the model using long term measurements of soil water content,
- analyzing annual course of energy and carbon balance components,
- testing the sensitivity of energy and carbon balance components to field capacity soil water content changes, and
- analyzing the statistical relationship between the energy, water, and carbon balance components.

In the following, these points are separately discussed after presenting the measurement site, the model, and the data used. At the end, basic conclusions are drawn.

2. Measurement site

The Agrometeorological Observatory of the University of Debrecen was established in 1962 at Hajdúhát (47°37'N, 21°36'E; 112 m asl). In the last 40 years period, both main climatic elements and the soil water content were systematically measured. This long time series of soil water content data is the

unique characteristic of the Observatory. The history of the Observatory and description of the measurements performed are given in *Szász* (2002).

The climate of Hajdúhát can be characterized as a temperate rainy climate with continental features. The annual mean temperature is 10.1°C, while mean annual precipitation sum is 550 mm. The water table is at a depth of 10 m. The soil type is lime covered with black loam (chernozem). The vegetation is short-cut natural grass.

3. Model and data

3.1. Inputs and outputs of the model

The input data are as follows: monthly precipitation (P), air temperature (T), sunshine duration (SSD) and $NDVI$ (normalized difference vegetation index), initial soil water content (Θ_{ini}), geographical latitude and longitude, albedo, and soil hydro-physical properties. Precipitation and temperature refer to the period 1953–2003, $NDVI$ (*Bartholy et al.*, 2004) and sunshine duration data refer to periods 1982–2000, 1971–2000, respectively. It is supposed that surface albedo changes from month to month, but there are no inter-annual changes. Soil hydro-physical properties are taken from *Ács et al.* (2005). The outputs are as follows: soil water content (Θ), potential evapotranspiration (PET), actual evapotranspiration (AET) or latent heat flux (LE), water surplus (S), water lack (D), soil respiration (SR), net primary productivity (NPP), net ecosystem exchange (NEE), radiation balance (R_n), sensible heat flux (H), and ground heat flux (G) (*Fig. 1*).

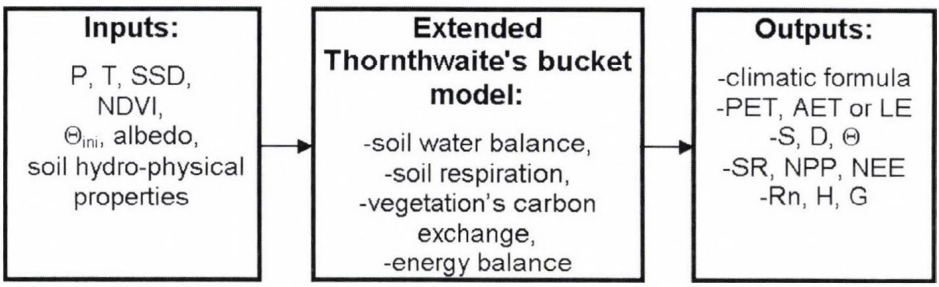

Fig. 1. Inputs and outputs of the extended Thornthwaite's bucket model. Symbols: P = precipitation, T = air temperature, SSD = sunshine duration, $NDVI$ = normalized difference vegetation index, Θ_{ini} = initial value of soil water content, PET = potential evapotranspiration, AET = actual evapotranspiration, LE = actual latent heat flux, S = water surplus, D = water demand, Θ = soil water content, SR = soil respiration, NPP = net primary productivity, NEE = net ecosystem exchange, R_n = net radiation flux, H = sensible heat flux, and G = soil heat flux at the soil surface.

Thornthwaite's bucket model (*Thornthwaite*, 1948) is extended by subroutines for calculating carbon and energy balance components of soil-vegetation system. Soil respiration is calculated according to *Peng et al.* (1998), while *NPP* after *Maisongrande et al.* (1995). The energy balance is calculated according to *Drucza* and *Ács* (2006).

3.2. Bucket model

The most simple soil water content prediction model is the bucket model. Bucket is represented by 1 m deep soil column of 1 m^2 surface which is filled by precipitation and depleted by *AET* and surface runoff. There is no water exchange between the column and the surrounding soil. Soil texture in the column is constant, that is, it has no horizontal and vertical changes.

3.3. Actual evapotranspiration

AET depends upon both the atmospheric conditions and Θ. Atmospheric conditions affect *PET*, while the effect of Θ is taken into account using the so-called β approach. The β function changes between 0 and 1, and it describes the dependence between the ratio *AET/PET* and Θ, that is

$$\frac{AET}{PET} = \beta(\Theta). \tag{1}$$

There are several methods to calculate both *PET* and β. In this study, *PET* is calculated after *Thornthwaite* (1948), while β after *Mintz* and *Walker* (1993).

3.3.1. Thornthwaite's parameterization of PET

Thornthwaite's method (1948) for parameterizing *PET* (mm $month^{-1}$) requires as input only monthly mean air temperature. A newer version of it is proposed by *McKenny* and *Rosenberg* (1993). It is as follows:

$$PET_i = 1.6 \cdot \left(\frac{L_i}{12}\right) \cdot \left(\frac{N_i}{30}\right) \cdot \left(\frac{10 \cdot T_i}{I}\right)^a, \tag{2}$$

where L_i is the average daytime length in hours for the ith month, N_i is the number of days in the ith month, and T_i is the monthly mean air temperature (°C) for the ith month. I is the thermal index calculated as:

$$I = \sum_{i=1}^{12} \left(\frac{T_i}{5}\right)^{1.514} \tag{3}$$

and

$$a = 6.75 \cdot 10^{-7} \cdot I^3 - 7.71 \cdot 10^{-5} \cdot I^2 + 1.792 \cdot 10^{-2} \cdot I + 0.49239. \quad (4)$$

AET's dimensions are equal to *PET*'s dimensions. In energy balance calculations, *LE* (MJ m^{-2} $month^{-1}$) is used instead of *AET* (mm $month^{-1}$).

3.3.2 Mintz and Walker's parameterization of β

Among many parameterizations of *β*, *Mintz* and *Walker*'s (1993) parameterization is used:

$$\beta(\Theta) = 1 - \exp\left(-6.8 \cdot \frac{\Theta - \Theta_w}{\Theta_f - \Theta_w}\right), \quad (5)$$

where Θ_w is the value of Θ at the wilting point and Θ_f is the one at the field capacity.

3.4. Carbon balance

3.4.1. Soil respiration

Annual sum of soil respiration is parameterized after *Peng et al.* (1998):

$$SR = 7.641 \cdot e^{0.0292 \cdot T} \cdot P^{0.171} \cdot AET^{0.4231}, \quad (6)$$

where *P* is the annual sum of precipitation, *AET* is the actual evapotranspiration, *T* is the mean annual air temperature (°C). Note that all relevant climatic elements are taken into account. Monthly sums of *SR* (10^{-3} kg C m^{-2} $month^{-1}$) are estimated after *Raich et al.* (1991) taking the effect of monthly mean air temperature and soil water content into account.

3.4.2. Net primary productivity

NPP is parameterized after *Maisongrande et al.* (1995):

$$NPP = \varepsilon \cdot R_g \cdot 0.5 \cdot NDVI \cdot (1 - r(T)), \quad (7)$$

where ε is the photosynthetic efficiency (10^{-3} kg MJ^{-1}), R_g is the monthly sum of global radiation (MJ m^{-2} $month^{-1}$), and $r(T_i)$ is the respiration of the vegetation expressed as a fraction of *NPP*. ε varies markedly, it depends upon vegetation type and geographical location. In this case, a constant value of $0.55 \cdot 10^{-3}$ kg MJ^{-1} is used.

3.5. *Numerical scheme*

Among many numerical schemes, a 2nd order implicit scheme was chosen. The set of equations is as follows:

$$\frac{\partial \Theta}{\partial t} = F(\Theta(t)), \tag{8}$$

$$\Theta_{t+1} = \Theta_t + [F_t + F_{t+1}] \cdot \frac{\Delta t}{2}, \tag{9}$$

where

$$F_t = P_t - AET_t, \tag{10}$$

that is

$$\Theta_{t+1} = \frac{\Theta_t + F_t - \frac{1}{2} \cdot \left.\frac{\partial F}{\partial \Theta}\right|_t \cdot \Theta_t \cdot \Delta t}{1 - \frac{1}{2} \cdot \left.\frac{\partial F}{\partial \Theta}\right|_t \cdot \Delta t}. \tag{11}$$

Euler-method has been used in every starting month. To stabilize the scheme, Θ_t has been averaged with new Θ in every time step, so Θ is in the next time step recalculated as:

$$\overline{\Theta}_t = \frac{\Theta_{t+1} + \Theta_t}{2}. \tag{12}$$

4. Results

Analysis is performed according to the points given in the introduction. Firstly, the performance of the bucket model is verified using measured Θ data from the Agrometeorological Observatory of the University of Debrecen, in the period 1972–1992. Then the annual course of simulated energy and carbon balance components is analyzed. Sensitivity of *SR* and *NEE* to Θ_f changes is also discussed. Lastly, statistical relationships between carbon and water balance components in the growing season are considered.

4.1. *Verification*

Temporal variation of measured and simulated Θ values obtained by the extended Thornthwaite's bucket model is presented in *Fig. 2a*. Agreement between simulated and measured Θ values is acceptable. According to the results, Θ values obtained by Thornthwaite's method are generally higher than

the measured ones. Overestimation is especially obvious in the spring. Correlation coefficient obtained is about 0.8.

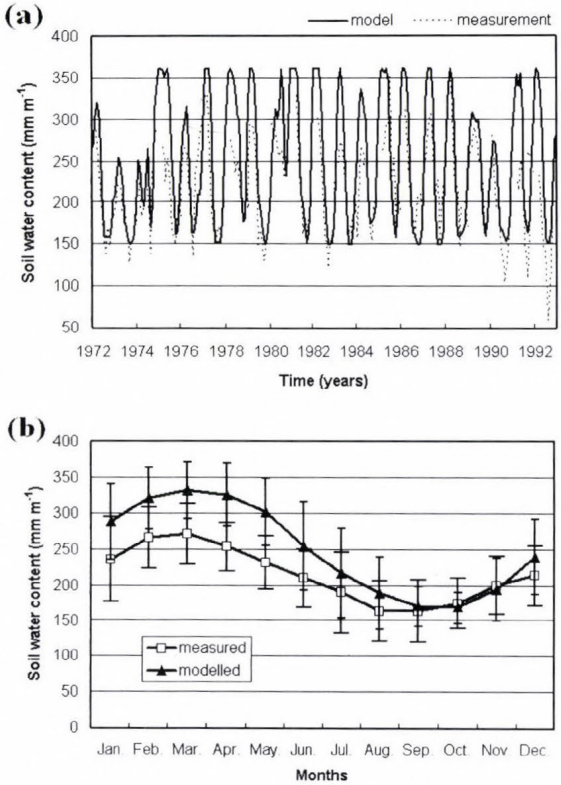

Fig. 2. Temporal variation of simulated and measured Θ obtained by the extended Thornthwaite's bucket model in the time period 1972–1992 (a). Long term mean annual course of simulated and measured Θ and its standard deviations (b).

Comparison of measured and simulated long term (1972–1992) mean annual course of Θ and its standard deviation are presented in *Fig. 2b*. Simulated values are in the scattering region of measured values $\Theta^{mea} - \sigma^{mea} < \Theta^{Thornt} < \Theta^{mea} + \sigma^{mea}$, except from February to May. $\Theta^{Thornt} - \sigma^{Thornt} < \Theta^{mea} < \Theta^{Thornt} + \sigma^{Thornt}$ relationship is also valid excepting spring. It should be said that difference between measured maximum and minimum Θ values changes between 120–260 mm m^{-1}. For modelled Θ values this range is between 80–210 mm m^{-1}.

4.2. Energy and carbon budget components

Long term (1971–2003) mean annual course of energy balance components is presented in *Fig. 3a*. R_n changes between –90 and +380 MJ m^{-2} $month^{-1}$, *LE*

between 0 and 270 MJ m^{-2} $month^{-1}$, while H between –80 and +150 MJ m^{-2} $month^{-1}$. LE is the highest in June because of the precipitation maximum, while it almost vanishes in January, when it amounts only 2 MJ m^{-2} $month^{-1}$. H is quite high in April (about 110 MJ m^{-2} $month^{-1}$), but it is the highest in August (about 150 MJ m^{-2} $month^{-1}$). Note that in October it is still positive (air is warmed by ground surface), but in November it is already negative. March is the month when the effect of the cold winter is over. Then air is usually warmer than the ground surface. Surface is wet ($\beta \approx 1$) but still cold because $R_n \leq LE$. This is obvious from the Bowen-ratio value, which is ~2.0 in this time period. In October, the Bowen-ratio is more than 0.5, which is also a high value for continental conditions. This is caused by macro-circulation effect, which appears regularly in the period September–October. This period is popularly called as 'indian summer'. G is negative in winter months and positive in summer months. Its annual sum is zero.

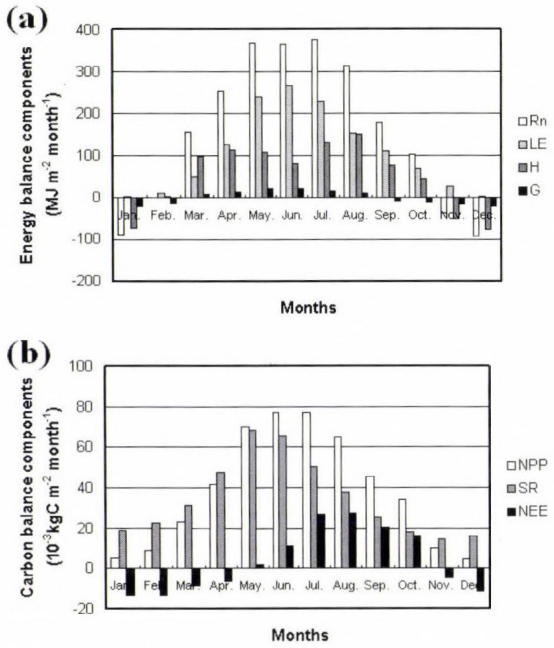

Fig 3. (a) Long term (1971–2003) mean annual course of radiation balance (R_n), latent heat flux (LE), sensible heat flux (H), and ground heat flux (G). (b) Long term (1982–2000) mean annual course of net primary productivity (NPP), soil respiration (SR), and net ecosystem exchange (NEE).

Long term (1982–2000) mean annual course of carbon balance components is presented in *Fig. 3b*. *NPP* and *SR* have similar courses, but their relation to each other is variable. This is reflected in *NEE* values. *NPP* is

the highest in July ($77 \cdot 10^{-3}$ kg C m^{-2} $month^{-1}$) and the lowest in December ($4 \cdot 10^{-3}$ kg C m^{-2} $month^{-1}$). *SR* is the highest in May ($68 \cdot 10^{-3}$ kg C m^{-2} $month^{-1}$). In November it amounts $14 \cdot 10^{-3}$ kg C m^{-2} $month^{-1}$. Note that *NEE* is negative in the period November–April, while it is positive in the period May–October.

4.3. Sensitivity analysis

Since Θ_f is an important parameter (*Ács*, 2005; *Ács et al.*, 2005) which depends upon soil type and climatic conditions, it is important to know how much it influences the energy and carbon balance components. The sensitivity analysis is performed by increasing/decreasing the Θ_f by ±10 percent with respect to its Θ_f^r value (Θ_f^r = 0.36 m^3 m^{-3}), which is used in verification tests. These Θ_f changes are not big, in reality Θ_f values can be scattered by about –45 – +15%. Runs performed by $\Theta_f^r = 0.36$ m^3 m^{-3} will be called as 'reference' runs.

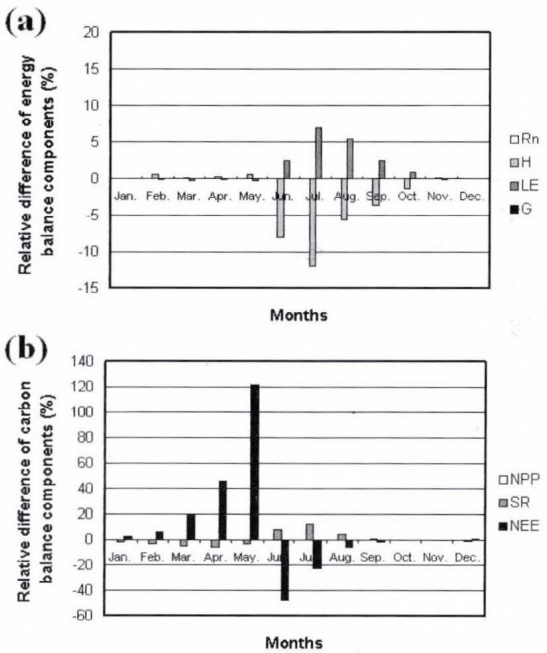

Fig. 4. Annual course of relative difference of energy balance (a) and carbon balance (b) components for $\Theta_f = \Theta_f^r - 0.1 \cdot \Theta_f^r$.

Annual course of relative differences of energy balance components for $\Theta_f = \Theta_f^r - 0.1 \cdot \Theta_f^r$ is presented in *Fig. 4a*. Deviations are small from January to May because of high Θ values (see *Fig. 2b*). In the period June–September, when evapotranspiration is higher than precipitation, Θ becomes important. Since Θ is lower than Θ^r, *LE* obtained is also lower than LE^r. Deviations of *H* in

some cases, however, exceed 10 percent as in June and July. In the autumn and winter periods, when *AET* is lower than *P*, relative deviations are small.

The same, but for carbon balance components, is presented in *Fig. 4b*. Relative deviations of *SR* follow the annual course of Θ. From January to April, relative deviations of *SR* with respect to SR^r are over 5 percent. From May to August, relative deviations are negative, in June and July they amount about –10 percent. In autumn, relative deviations are small. Nevertheless, deviations of *NEE* are higher and even reversed to deviations of *SR*. For positive deviations of *SR*, *NEE* deviations are negative and vice versa. In extreme cases, as in April, May, and June, *NEE* deviations amount about –40, +100 and +60 percent, respectively. *NEE* changes are bigger, because *NEE* values are lower than *SR* and/or *NPP* values.

Annual course of relative deviations of energy and carbon balance components for $\Theta_f = \Theta_f^r + 0.1 \cdot \Theta_f^r$ is presented in *Fig. 5a* and *Fig. 5b*, respectively. Relative deviations in absolute value are about the same as in the former case but, courses are opposite. Note that high relative deviations of *NEE* are high again. Summarizing: 10 percent changes in absolute value of Θ_f^r resulted about 5–10 and 50–100 percent changes in absolute values of LE^r and NEE^r, respectively.

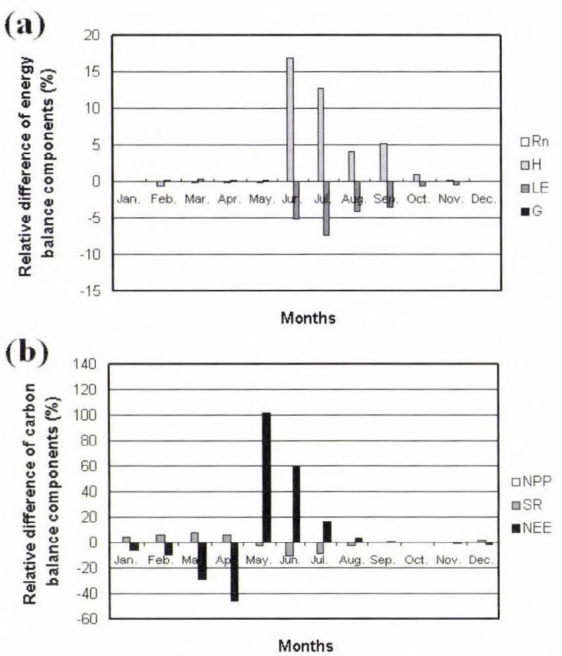

Fig. 5. The same as in Fig. 4a, but for $\Theta_f = \Theta_f^r + 0.1 \cdot \Theta fr$ (a). The same as in Fig. 4b, but for $\Theta_f = \Theta_f^r + 0.1 \cdot \Theta_f^r$ (b).

4.4. Statistical relationships between carbon balance components and environmental factors in the growing season

The period March–November will be called as growing season (GS). This time period is interesting because of the activity of both the soil and vegetation. In this period carbon balance components are significantly changing. There is a strong relationship between *SR* and *H* (see *Fig. 6a*). The correlation coefficient is 0.91. *SR* values are scattered between 300–450 10^{-3} kg C m^{-2} GS^{-1} and sensible heat flux changes between 300–1150 MJ m^{-2} GS^{-1}. Relationship between *NEE* and Θ is presented in *Fig. 6b*. The correlation coefficient is –0.76, that is, *NEE* increases by decreasing of Θ. *NEE* changes between 16 and 160 10^{-3} kg C m^{-2} GS^{-1}. Somewhat stronger relationship exists also between *NEE* and *H* (see *Fig. 6c*). The correlation coefficient is 0.8, that is, *NEE* increases by increasing *H*.

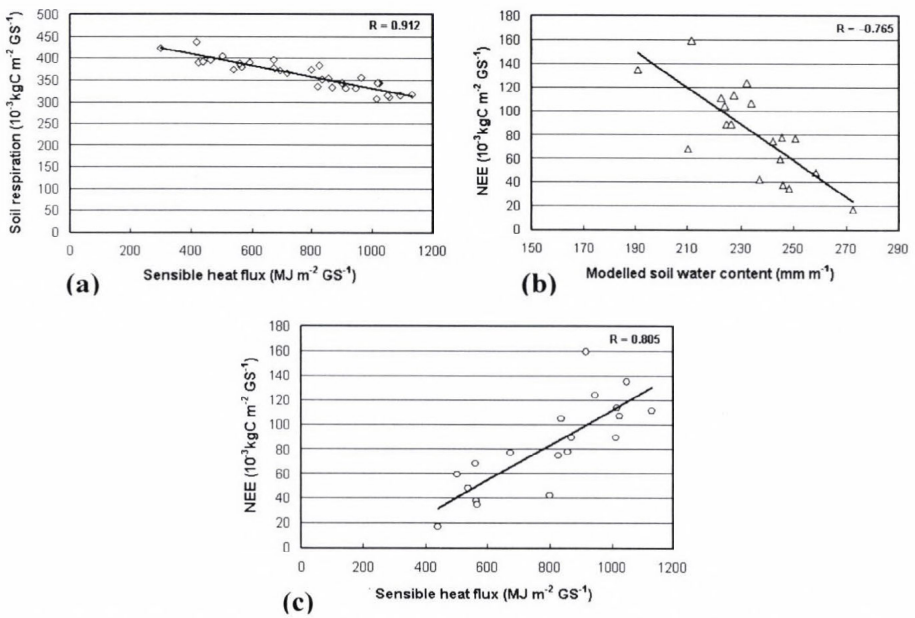

Fig. 6. Statistical relationship between (a) the soil respiration and sensible heat flux, (b) the net ecosystem exchange and precipitation, (c) the net ecosystem exchange and sensible heat flux in the growing season.

5. Conclusions

An extended Thornthwaite's bucket model is applied for estimating surface energy and carbon balance components in the vicinity of Debrecen. Soil water prediction module of the model is verified using measured Θ data from the Agrometeorological Observatory of the University of Debrecen, in the period

1972–1992. There are no verification tests referring to energy and carbon balance components because of the missing direct measurements. Long term mean annual course of energy and carbon balance components is analyzed as well. The sensitivity of *NEE* to Θ_f changes and statistical relationships between energy and carbon balance components in the growing season are considered too.

It is shown that energy balance components are quite influenced in the period September–October (this period is popularly called as 'indian summer'). In this period *Péczely*'s (1961) 12th macro-circulation pattern type is dominating. It is also shown that *AET* and carbon balance components are strongly coupled. Since *AET* is strongly determined by Θ_f, *SR* and/or *NEE* are also sensitive to the changes of Θ_f. In some cases sensitivity of *NEE* to Θ_f could be extremely high. Note that Θ_f is a roughly estimated parameter (*Ács*, 2005). Of course, *NEE* depends not only upon Θ_f, but also upon ε. In our case ε is taken to be 0.55 10^{-3} kg MJ^{-1}. *NEE* values obtained should be treated with caution, because both ε and Θ_f are quite unknown and variable parameters. The model applied does not use any upscaling procedure. Area and time variability of environmental conditions is only implicitly represented by the input data. Thus, model outputs are area and monthly averages, just as the inputs.

References

Ács, F., 2005: On transpiration and soil moisture content sensitivity to soil hydrophiysical data. *Bound.-Lay. Meteorol. 115*, 473–497.

Ács, F., Szász, G., and *Drucza, M.*, 2005: Estimating soil moisture content of a grass-covered surface using an energy balance approach and agroclimatological observations. *Időjárás 109*, 71–88.

Bartholy, J., Pongrácz, R., Barcza, Z., and *Dezső, Zs.*, 2004: Aspects of urban/rural population migration in the Carpathian basin using satellite imagery, 289–313. In *Environmental Change and Its Implications for Population Migration* (eds.: *J.D. Uruh, M.S. Krol*, and *N. Kliot*). Kluwer Academic Publishers, 313 pp.

Drucza, M. and *Ács, F.*, 2006: Relationship between soil texture and near surface climate in Hungary. *Időjárás 110*, 135–153.

Justyák, J., and *Tar, K.*, 1994: *Debrecen's Climate* (in Hungarian). KLTE, Debrecen, Hungary, 160 pp.

Maisongrande, P., Ruimy, A., Dedieu, G., and *Saugier, B.*, 1995. Monitoring seasonal and interannual variations of gross primary productivity, net primary productivity and net ecosystem productivity using a diagnostic model and remotely-sensed data. *Tellus 47B*, 178–190.

Mckenny, M.S. and *Rosenberg, N.J.*, 1993: Sensitivity of some potential evapotranspiration estimation methods to climate change. *Agr. Forest Meteorol. 64*, 81–110.

Mintz, Y. and *Walker, G.K.*, 1993: Global fields of soil moisture and land surface evapotranspiration derived from observed precipitation and surface air temperature. *J. Appl. Meteorol. 32*, 1305–1335.

Péczely, Gy., 1961: Climatological characterization of the macrosynoptic types of Hungary (in Hungarian). *Országos Meteorológiai Intézet Kisebb Kiadványai, 32*, Budapest.

Peng, C.H., Guiot, J., and *van Campo, E.*, 1998. Past and future carbon balance of European ecosystems from pollen data and climatic models simulations. *Global Planet Change 18*, 189–200.

Raich, J.W., Rastetter, E.B., Melillo, J.M., Kicklighter, D.W., Steudler, P.A., and *Peterson, B.J.*, 1991: Potential net primary productivity in South America: Application of a global model. *Ecol. Appl. 1*, 399–429.

Szász, G., 2002: Energy budget between the atmosphere and surface in the vegetation period during 1963–1994. *Időjárás 106*, 161–184.

Thornthwaite, C.W., 1948. An approach toward a rational classification of climate. *Geogr. Rev. 38*, 5–94.

IDŐJÁRÁS

Quarterly Journal of the Hungarian Meteorological Service
Vol. 111, No. 4, October–December 2007, pp. 251–260

A case study on the relationship between radiation intensity and stomatal conductivity in fragmented reedbeds

Angéla Anda[1,*], **Ferenc Horváth**[2], **Anett Boldizsár**[1] and **László Erdei**[2]

[1]*Department of Meteorology and Water, Faculty of Agronomy, Pannon University*
P.O. Box 71, H-8361 Keszthely, Hungary; E-mail: anda-a@georgikon.hu

[2]*Department of Plant Physiology, University of Szeged,*
P. O. Box 654, H-6701 Szeged, Hungary

(Manuscript received in final form January 19, 2007)

Abstract—Despite the fact that a large number of papers have dealt with the causes of reed die-back, little attention has been paid to the probable effect of environmental factors. Fragmentation is an early sign of die-back and is associated with a considerable change in the environment, particularly in the intensity of radiation. In the present study the relationship between radiation and stomatal conductivity was examined in reeds growing in non-fragmented and fragmented stands on the northern shore of Lake Balaton (Hungary). Hourly measurements were made on the adaxial and abaxial leaf surfaces at every leaf storey of selected shoots on sampling days with the same solar angle in June 1999.

The greater exposure of the fragmented stands to radiation would have been expected to lead to enhanced stomatal conductivity, as plants standing in the lake did not suffer from water deficiency, but this was not the case. The conductivity of plants in the fragmented stand was found to be around 20% lower than that of reeds in a non-fragmented stand, though the direction of the change differed on the two surfaces of the leaves. An intense reduction in conductivity was observed on the adaxial surface and a more moderate increase on the abaxial surface. This discrepancy was greatest at dawn and at a high solar angle. This is thought to be due to adaptation to the stress caused by changes in the environment – more intensive radiation penetration, higher air temperature, reduced humidity – to which the plants in fragmented stands are exposed. Decreased conductivity of fragmented plants results in reduced CO_2 uptake and probably less carbon assimilation as well. This might be one of the reasons leading to reed deterioration of fragmented stands.

A comprehensive analysis of the microclimate of reeds growing in non-fragmented and fragmented stands will be essential if a more detailed picture is to be obtained of changes in stomatal conductivity.

Key-words: fragmented reed, stomatal conductance, radiation relation

* Corresponding author

1. Introduction

Reeds, one of the most frequent aquatic plants in the Balaton region, play an important role in maintaining the quality of the lake water. The die-back of reeds has become a major problem in the Balaton area in recent decades. In spite of the considerable efforts that have been made to discover the possible reasons for reed decline, the results so far have been modest. It is frequently observed in nature that reedbeds undergo changes in water supply from time to time, becoming temporarily dry or completely inundated with water. However, fragmentation, rather than the continuous variability in the water level, may be the first sign of reed decline. Observations on the die-back of reed stands were published earlier by *Van der Putten* (1997) for reedbeds in central and eastern Europe, and by *Erdei et al.* (2001) for reedbeds in the lake Balaton area. An unusual extent of reed decline, exceeding anything previously recorded, was also observed by *Fogli et al.* (2002) in the Sub-Mediterranean region. *Ostendorp et al.* (2003) attempted to explain the causes of the deterioration of reed stands from 41 lakeshores in central Europe and concluded that lake eutrophication cannot be regarded as the general reason for reed die-back in eastern Europe.

In 1998 the number of fragmented reedbeds isolated from the main stands increased dramatically in Lake Balaton, so tests were made in summer 1999 to determine the difference in radiation intensity compared with that reaching untouched reedbeds and to investigate how fragmented reedbeds, which represent the first symptom of reed die-back, adapt to changes in radiation intensity and related changes in stomatal conductivity. This latter parameter provides direct information on the evapotranspiration of plants standing in water, which is determined solely by the radiation intensity. The results of these observations could contribute to a better understanding of the complex process of reed die-back, and particularly of its relationship to environmental changes.

2. Materials and methods

Observations on the radiation intensity in nonfragmented reed stands in Lake Balaton and in fragmented but still viable reedbeds separated from the main stand were carried out in the neighborhood of Balatonfűzfő in June 1999, together with measurements of stomatal activity. The choice of sampling date and place was justified by the increasing number of fragmented reedbeds. At the beginning of the experiment four treatments were distinguished. Reedbeds with a nonfragmented canopy were taken as the control (designated as *E*), while fragments separated from the main stand were classified on the basis of the shoot number. The smallest fragments contained 25–50 shoots, the next category contained around 100 shoots, and the third group consisted of 130–150 shoots. However, as the three groups gave similar responses to the radiation parameters

tested, this classification proved unnecessary, so all the fragments were considered as a single treatment (designated as *B*).

The effect of radiation on the stomatal conductivity of reeds in the vegetative phase of development, with an average of 4–10 leaf layers, was recorded on consecutive days in order to eliminate the modifying effect of differences in the solar angle on the relationship between radiation and stomatal conductivity. The investigation of this relationship was favored by the development of fragmented reedbeds, as it allowed the effect of two levels of radiation intensity to be observed simultaneously.

In 1999 a number of cloudy days occurred after June 20, so days were chosen that were uniformly overcast, which meant that there were no great fluctuations in radiation intensity. The completely overcast, "average" sampling day produced from observations made over several days in late June had no previous equal in the literature, except as an explanation for deviations in stomatal activity for brief periods on otherwise bright days. The diurnal variation in stomatal conductance is illustrated by the data of hourly sampling with three repetitions. Parallel with diurnal variation investigations, in contrast to the usual measurements of stomatal conductivity, made on a single, well-illuminated leaf layer, in some cases the present measurement was extended to include all the leaf layers and the conductivity was recorded on both the upper (g_u) and the lower (g_l) epidermis (vertical profiles). According to *Larcher* (2001), the conductivity of the whole leaf (g) can be determined on the analogy of parallel-connected resistances (the reciprocal of conductivity) on the two sides of the leaf. The mean value for each shoot was calculated from the conductivity of all the leaves (series-connected). In vertical profile investigations, in contrast to daily variation, the number of repetitions was ensured not by multiple samplings on a single leaf layer but by measurements on all the leaf layers on the shoot (*Erdei et al.*, 2001). Beside the average values, the coefficient of variation (*CV*, %), and the standard deviation relative to the mean were included in the analysis.

The measurement of radiation was carried out simultaneously with that of stomatal conductivity using a quantum sensor used for the determination of photosynthetically active radiation (*PAR*, μmol s^{-1} m^{-2}). The number of repetitions was the same as in stomatal conductance. The instrument employed was a DELTA T AP4 transient porometer containing sensors for recording both radiation and stomatal conductivity.

3. Results

3.1. Relationship between the radiation and stomatal conductivity

In addition to biological traits, the stomatal conductivity (reciprocal of stomatal resistance) is determined primarily by environmental factors: by the water

supplies, representing the hygric component, and by radiation, which provides energy. In the case of reeds standing in water, radiation becomes the primary determinant of stomatal conductivity. The radiation opens the pore in the morning. Later on, when the water is not limiting factor, the higher the radiation intensity, the more opened the stomata. The other abiotic meteorological elements, such as air temperature, air humidity, wind characteristics also affect the movement of the stomata. We have got much less information about the influence, mainly the mechanism of the biotic factors on stomatal behavior. Earlier study on maize showed that diseased plants have higher surface temperature ("fewer") resulted of an increased stomatal resistance referring to decaying the water balance of healthy plants (*Anda*, 1993, 1994). Every factor, biotic or abiotic that increases the stomatal resistance, reduces the input of CO_2 and damages the process of photosynthesis. These disturbances may effect negatively the final production of plants independently on their species, age or phenological phase. In the time of our measurements both the fragmented and nonfragmented reed stands were free from biotic stresses.

The conductivity of healthy and fragmented reedbeds responded differently to variations in radiation intensity (*Fig. 1*). In reedbeds with nonfragmented canopy, *PAR* intensity in excess of 1500 μmol m^{-2} s^{-1} was rarely recorded. Fragmented reedbeds, however, were more open to the environment, so higher *PAR* values were observed, which also allowed examinations to be made over a wider radiation range. For reedbeds with a nonfragmented canopy, the upward slope of the curve describing the relationship between light and stomatal conductivity was steeper above a radiation level of 400 μmol m^{-2} s^{-1} (morning hours) than for fragmented reedbeds, indicating that in a nonfragmented stand the plants responded to unit increase in radiation intensity by greater stomatal opening. The beginning of stomata closure was at 400 μmol m^{-2} s^{-1} light intensity in the time of our experiment.

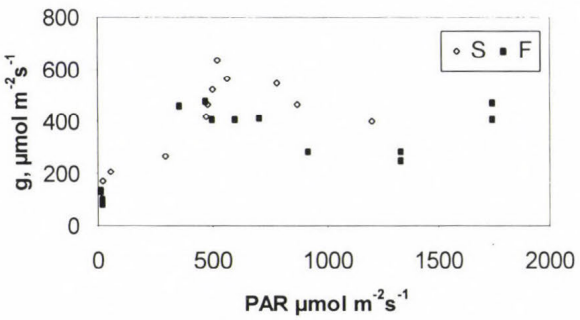

Fig. 1. Relation in photosynthetically active radiation (*PAR*) and stomatal conductance (*g*) of fragmented reed canopy. *S* denotes values for nonfragmented reed stands, *F* denotes values in the fragmented patches. The number of measurements is 24.

The radiation environment of small isolated reedbeds was modified considerably. They received more uniform radiation, but were more exposed to wind and waves than plants within a nonfragmented stand. The modification in the environment and microclimate (radiation penetration, inside air temperature and air humidity, wind) as the result of fragmentation may act as a stress factor, especially at the beginning of the acclimatization period, and may also influence the stomatal conductivity.

Diurnal changes in the stomatal conductivity of nonfragmented reed canopies and fragmented reedbeds in Lake Balaton on bright days were reported by *Erdei et al.* (1998). In agreement with earlier results by this author, the maximum conductivity occurred in both types of reedbeds at around 11 a.m., shortly before the maximum value of radiation (PAR = 600–700 μmol m^{-2} s^{-1}). After a transitional decline, possibly associated with stomatal closure at around noon (*Anda* and *Boldizsár*, 2005), there was a further, more moderate increase at radiation values in excess of PAR = 1500 μmol m^{-2} s^{-1}.

No difference was observed in the mean stomatal conductivity of each shoot in fragmented reedbeds with different shoot numbers (density). The mean leaf conductivity (recorded on the adaxial and abaxial surfaces) in the fragmented groups decreased by 21% compared with the healthy stand. In fragmented treatments the increase in coefficient of variation was 10%. At low solar angle the difference between the two treatments was less pronounced (13%) (*Fig. 2*). The greater radiation reaching the plants in the more open fragmented stands, which were also more exposed to the wind, while the water supplies were unchanged, would have been expected to cause an increase in stomatal conductivity, while in reality the opposite was observed, probably due to the radical change in the plant environment in the fragmented stands, which can be assumed to be less favorable to the plants than a nonfragmented reedbed. Earlier studies on other plant species demonstrated that environmental stress, whether biotic (fungus, insects, viruses, bacteria) or abiotic (lack of N-fertilizer, water shortage) led to an increase in stomatal resistance (*Anda* and *Lőke*, 1997), i.e., to a reduction in stomatal conductivity.

In fragmented reed difference occurs not only in the magnitude of adaxial and abaxial conductivity, but also in the direction of modification compared with the average value for plants within a reedbed. The reduction in mean conductivity per shoot on the adaxial leaf surface of reed stands was extremely large in the early morning and late afternoon, being around 42–49%. At the same time the conductivity on the abaxial surface of reed stand leaves rose by 14.7–32% (*Fig. 3*). The stomata of the lower epidermis also exhibited greater sensitivity at low solar angle. It should be noted, that this rise in conductivity on the abaxial surface of fragmented reeds was only observed for all leaf zones at certain radiation intensities. One such solar angle was immediately after sunrise at PAR = 15–20 μmol m^{-2} s^{-1}, when the difference between the fragmented stands and healthy reedbeds was as much as 150–200%. At high solar angle,

with *PAR* values of 1200–1600 μmol m^{-2} s^{-1}, the increase in stomatal conductivity was also substantial (152–173%). At other solar angles there was always one leaf zone in the vertical profile, where the abaxial conductivity of the fragmented reed did not follow the trend for the shoot as a whole.

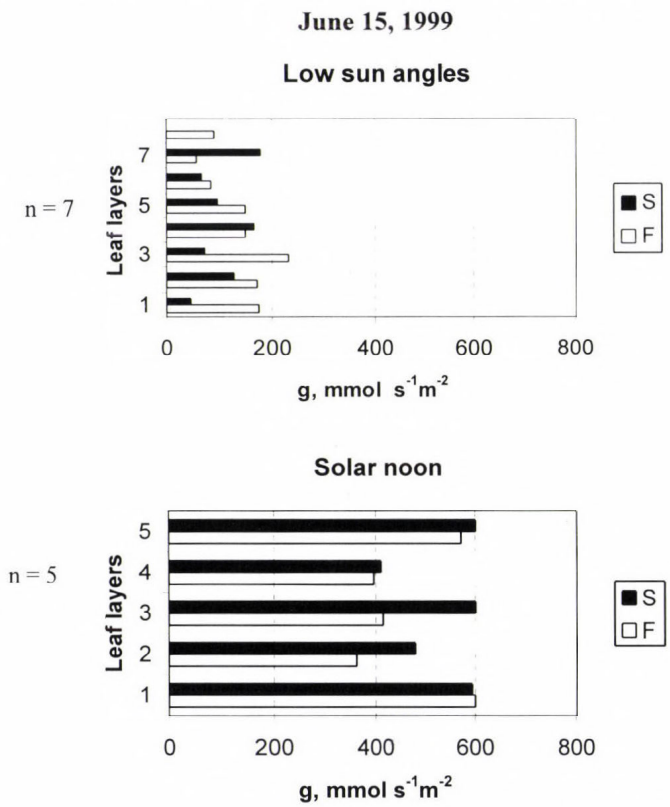

Fig. 2. Vertical profiles of the leaf stomatal conductance (*g*) at low (*PAR* = 20 μmol m^{-2} s^{-1}, leaf temperature = 17.7°C) and high solar radiations (*PAR* = 495 μmol m^{-2} s^{-1}; leaf temperature = 23.4°C). *S* denotes the values for healthy stand and *F* is for the fragmented reeds. *n* denotes the number of measurements.

According to earlier observations on the effect of changes in the radiation environment, which can be expected to have been modified in the case of fragmented reeds, factors causing short-term changes deserve the greatest attention. These deviations in radiation induce an acclimatization response in the plants, e.g., a change in leaf thickness, the occurrence of biochemical reactions, or simply a change in leaf movement, etc. (*Larcher*, 2001). Considering the exceptional sensitivity of the stomata to environmental factors, the greater leaf movement caused by the wind in more open stand and the resulting increase in exposure may be sufficient to cause a modification in the stomatal movement.

The higher mean value calculated from the abaxial conductivity recorded for each leaf zone on the shoots of fragmented reeds was characteristic in 94.7% of the total investigations.

In the shoots of healthy reedbeds an increase in conductivity was observed on the abaxial surface compared with the adaxial surface in 43.7% of the cases, though this difference was generally very slight during the day. Even considering the great variability of stomatal conductivity, this difference is noteworthy. The fact, that these changes are masked in some cases in mean stomatal conductivity values, can be explained by the high level of uncertainty caused by point sampling errors. According to *Pearcy et al.* (1991), the measuring error of observations on stomatal activity using a porometer may be as much as 30% or more.

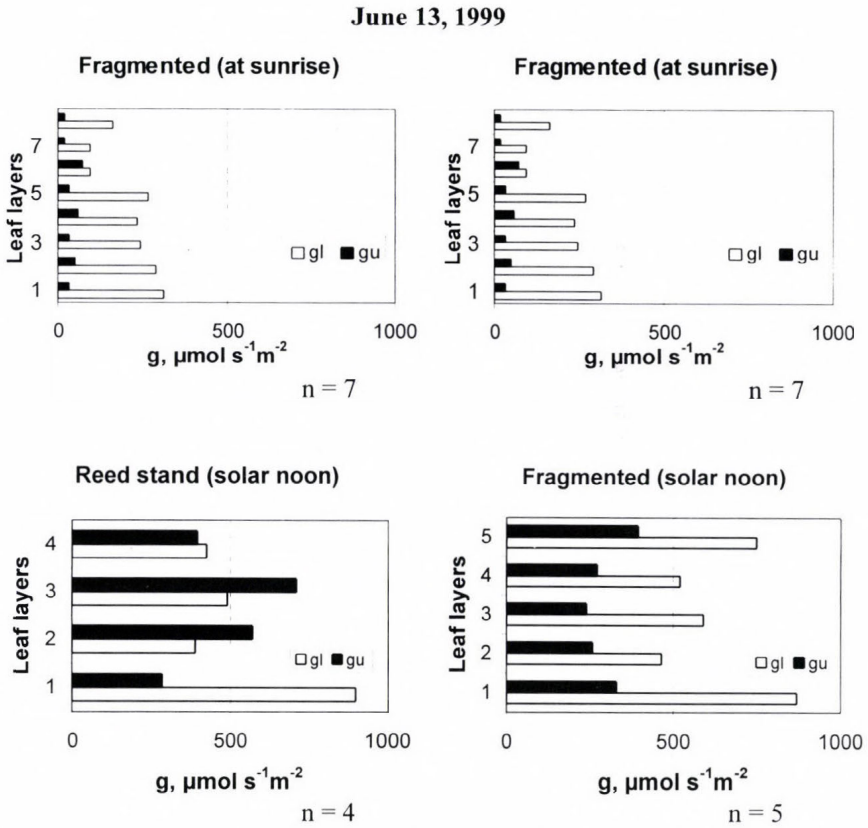

Fig. 3. Vertical profiles of the stomatal conductance on the lower (g_l) and upper (g_u) epidermis. In the time of sunrise *PAR* is 15–50 µmol s^{-1} m^{-2} and leaf temperature is 17.8–18 °C. In the solar noon *PAR* is 1300–1530 µmol s^{-1} m^{-2} and the leaf temperature is 23.4–25 °C. *n* denotes the number of measurements.

3.2. Stomatal conductivity of reeds on sampling days with even cloud cover

Irrespective of the plant species, studies on stomatal activity are generally carried out on bright, clear days due to the difficulties encountered during the measurements. Results obtained for healthy and fragmented reedbeds in Lake Balaton were reported by *Erdei et al.* (1998). Due to the variability of the weather, however, it may also be necessary to investigate the stomatal activity when the weather is overcast. This is not possible for all types of cloud cover. In the present study days were chosen, when the cloud cover ensured relatively uniform radiation, allowing the successful measurement of conductivity. The samples were taken at the end of June, during the period immediately following the bright sample days, at the same solar angle. In the early morning hours the reeds were wet, making them unsuitable for measurements, so the diurnal changes are illustrated using values recorded every hour between 10 am and 4 pm. As in the case of values calculated in clear weather, the hourly values are the mean of the conductivity measured on the abaxial and adaxial surfaces.

The stomatal conductivity values recorded on cloudy days were considerably lower than those measured on bright days (*Fig. 4*). The actual value is always determined by the radiation intensity (*PAR*), which fluctuated between 20 and 335 μmol m^{-2} s^{-1} during the observations. The measurements indicated that a *PAR* value of approx. 10–15 μmol m^{-2} s^{-1} is required for the stomata to open, and the lowest conductivity that can be measured is around 25–30 μmol m^{-2} s^{-1}. The change in the cloud cover is revealed by the apparently random stomatal conductivity values, which varied from hour to hour and, despite the low diurnal means 90.6 and 94.7 μmol m^{-2} s^{-1} in nonfragmented reed canopy and fragmented plants, had a relatively high coefficient of variance (*CV* is 68%), half as much again as that found on bright days.

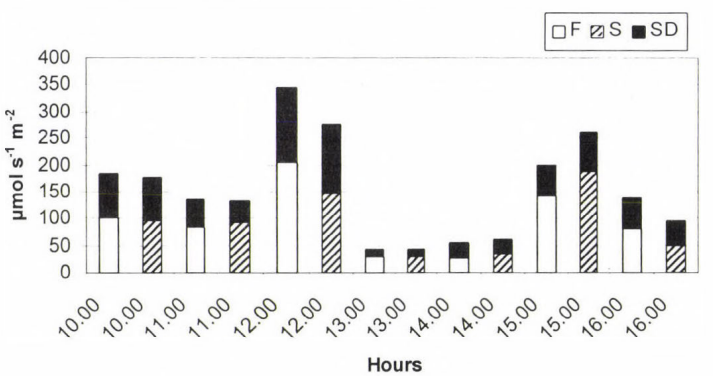

Fig. 4. Daily variation in the stomatal conductance of reed on overcast day. The mean of the measurements in nonfragmented reed stand (*S*) and fragmented treatment (*F*) were 90.6 and 94.7 μmol s^{-1} m^{-2}, respectively. *SD* designates standard deviation.

Unlike the results obtained on bright days, no differences in stomatal conductivity were observed on dull days between the healthy and fragmented reedbeds.

4. Discussion and conclusions

The radiation sensitivity of the stomata during the vegetative phase of development differs in healthy and fragmented reedbeds. Reeds in a healthy stand responded to an increase in unit radiation intensity during the morning hours with greater conductivity. Fragmented reedbeds, which were completely open to the elements, were less sensitive to radiation, probably because they had become acclimatized to radiation stress. Stomatal closure followed by renewed stomatal opening was only observed occasionally in fragmented stands at a very high level of radiation. Light intensity measurement within nonfragmented stand was never higher than 1500 $\mu mol\ m^{-2}\ s^{-1}$ in June 1999.

The daily mean leaf conductivity (recorded on the adaxial and abaxial surfaces) in the fragmented groups decreased by 21% compared with the healthy stand. In fragmented treatments the increase in coefficient of variation was 10%. This result was unexpected. For fragmented stands more exposed to radiation, the conductivity should theoretically increase for plants standing in the lake, where water supplies are not a limiting factor. This unexpected phenomenon can probably be attributed to a radical change in the microclimate of the surrounding fragmented stands. For reeds previously growing in a nonfragmented stand, fragmentation inevitably results in intense abiotic stress. In the time of our measurements the fragmented reed was free from biotic stresses.

The direction of difference in stomatal conductivity in fragmented reedbeds differed on the abaxial and adaxial leaf surfaces. While a reduction in conductivity was recorded on the adaxial leaf surface of plants in fragmented stands, an increase was measured on the abaxial surface, compared with plants in nonfragmented stands. At dawn, at low rates of radiation, and at noon, when the radiation was intense, this was true of all the leaf zones. In the intermediate hours changes of opposite sign were observed for some leaf storeys. In daily averages the decreased conductivity of fragmented plants could result reduced CO_2 uptake and carbon assimilation. Among others, disturbance of process of photosynthesis might be one of the reasons leading to reed deterioration of fragmented stands. Our sample day was in the beginning of reed vegetation period (end of June) showing moderate problems in stomatal behavior. Later on this inconvenience intensified in fragmented reed patches, mainly in the following season, ending with complete die-back of plants.

As expected, the mean stomatal conductivity on a sampling day with even cloud cover in late June was lower than in bright weather, with a high coefficient of variance. On cloudy days fragmentation had no influence on trends in the stomatal conductivity of reeds.

The causes of reed die-back in Lake Balaton, which has been detected for some time, are extremely complex. Many scientists attribute the die-back to the simultaneous appearance of a number of unfavorable factors. The present paper was not designed to investigate all the causes, but attempted to shed light on the enhanced sensitivity of fragmented reeds to radiation. The results suggest that complex analysis involving not only radiation but also other factors in the microclimate will be required if we are to understand the changes in stomatal conductivity observed in fragmented reedbeds.

Acknowledgements—This work was supported by the Hungarian Scientific Research Foundation (OTKA T 032524).

References

Anda, A., 1993: Surface temperature as an important parameter of plant stand. *Időjárás 97*, 259-269.

Anda, A., 1994: Infrared thermometry: A new tool in detecting plant diseases (in Hungarian). *Proc. on Forum in Plant Protection*, Keszthely (Hungary), 27 January, 1994.

Anda, A. and *Lőke, Zs.*, 1997: Use of stomatal resistance: Theory and practice. *Annales Geophysicae.* Part II. Supplement II, *15*, p. 288.

Anda, A. and *Boldizsár, A.*, 2005: Transpiration and plant surface temperatures of reedbeds with different watering levels. *Georgikon for Agric. 8*, 39-52.

Erdei, L., Szegletes, Zs., Horváth, F., and *Pécsváradi, A.*, 1998: Changes in ion accumulation, stomatal movements and nitrogen metabolism in clonal fragments of the common reed, Phragmites australis (Cav.) Trin. ex Steudel in the Lake Balaton. In *Proc. of the 11th Congress of the Federation of European Societies of Plant Physiology (FESPP)*. Varna, Bulgaria. *Bulgarian J. Plant Physiol.* (special issue).

Erdei, L., Horváth, F., Tari, I., Pécsváradi, A., Szegletes, Zs., and *Dulai, S.*, 2001: Differences in photorespiration, glutamine synthetase and polyamines between fragmented and closed stands of Phragmites australis. *Aquat. Bot. 69*, 165-176.

Fogli, S., Marchesini, R., and *Gerdol, R.*, 2002: Reed (Phragmites australis) decline in a brackish wetland in Italy. *Mar. Environ. Res. 53*, 465-479.

Larcher, W., 2001: *Physiological Plant Ecology*. Springer Verlag, Berlin-Heidelberg-New York, 513 pp.

Ostendorp, W., Dienst, M., and *Schmieder, K.*, 2003: Disturbance and rehabilitation of Lakeside Phragmites Reeds following an extreme flood in Lake Constance (Germany). *Hydrobiologia*, No.1-3, 687-695.

Pearcy, R.W., Ehleringer, J., Mooney, H.A., and *Rundel, P.W.*, 1991: *Plant Physiological Ecology*. Chapman and Hall, London-New York-Tokyo, 457 pp.

Van der Putten, W., 1997: Die-back of Phragmites australis in European wetlands: An overview of the Research Program on Reed Die-back and Progression (1993-1994). *Aquat. Bot. 59*, 263-275.

IDŐJÁRÁS

Quarterly Journal of the Hungarian Meteorological Service
Vol. 111, No. 4, October–December 2007, pp. 261–279

Diurnal course of potential wind power with respect to the synoptic situation

Károly Tar

Department of Meteorology, Faculty of Science, University of Debrecen, P.O. Box 13, H-4010 Debrecen, Hungary; E-mail: tark@puma.unideb.hu

(Manuscript received in final form June 7, 2007)

Abstract—This study is a segment of complex wind energy examinations, which uses statistical methods to analyze the daily mean specific wind power of a month in the period between 1991 and 2000 on seven Hungarian meteorological stations. The properties of monthly average specific wind power can be examined by the definite integral of an approximation function fitting the hourly average of the cubes of wind speed. Certain properties of the approximation function will be analyzed in this paper, mainly its periodicity that may offer implications about the daily course of wind energy. Relations of periodicity of daily course with weather situations are also investigated. Thus, we outline a statistical, stochastic-climatologic model, which could be utilized by energetic systems management in producing electricity from wind energy.

Key-words: average specific wind power, trigonometric polynomials, relative amount of approximation, suddenness and periodicity of the approximation function, weather situations

1. Introduction

In a given term consisting of days (e.g., month, season), the daily average specific wind power is estimated with the definite integral (area under the curve) of a trigonometric polynomial matching the hourly averages of the cubes of wind speeds. In this way, the dependence on the number of measurement times is eliminated, on the other hand, we can investigate the daily courses of wind power: they are the 24-hour and the 12-hour periods in the case of the first two members of trigonometric polynomials. As it is known, the temporal alternation of potential wind power is extremely inconvenient for the operation of electricity, for the power loss must be substituted from other sources. The greatest daily difference may exceed 80% in Germany (*Stróbl,* 2006). For electric energy production those days are advantageous, when the daily (24-hour) course of

hourly average wind speed cubes is a simple one with only a single maximum. Days, when the second wave (12-hour period) is random, always have simple daily course with a single maximum. Accordingly, our investigations are applied primarily to the 12-hour period. Only the relationship with the weather situations of the always present whole day period is analyzed in detail.

2. *Objective and database*

The paper discusses a segment of a complex examination, the objective of which is to reveal the inter-dependence of parameters in wind energy in order to outline a statistical, stochastic climatologic model that may be useful in everyday wind energy utilization.

Specific wind power (P_f , in W m^{-2}), is defined as the kinetic energy of the air mass passing through a unit of vertical area in a unit of time. We can calculate it at any given time with the formula

$$P_f = \frac{\rho}{2} v^3, \tag{1}$$

where v is the velocity of wind, ρ is the air density. There are two options to determine the specific wind power of an extended period: either we substitute for the average speed of the period or we add wind power values defined at individual discrete points in time within the period in question. The second option is obviously more realistic. It is problematic, though, that in this case the sum depends on the number of measurement times, as different values are obtained when calculated from wind speeds measured in every hour, in every ten minutes, or at the so called terminal points each day. Although averaging might reduce the dependence on the number of measurement points, it cannot entirely eliminate the problem.

There is a theoretical solution to eliminate this dependence. When the area under the curve of the function describing daily variation in the cubes of wind speeds is multiplied by $\rho/2$, the exact value of every daily specific wind power is obtained. We must use numerical integration, as the necessary function is not analytic on a usual day. We may attempt to determine the average specific wind power falling on a period consisting of days, for instance month, season, or year with an appropriate approximation function.

Hourly wind speed data of ten Hungarian meteorological observatories in the period from 1991 to 2000 required for the energetic examination were provided by the Hungarian Meteorological Service. *Fig. 1* shows the geographical location of the stations. The weather stations in Debrecen, Békéscsaba, Miskolc, and Győr, which are not restricted to wind speed examinations, were relocated (at least once) in the period from 1991 to 2000 of the comprehensive study. The relocation did not caused substantial change in the latitudes or longitudes of any

stations concerned, however, increased the elevation in Miskolc and the anemometer height in Békéscsaba. Both heights were changed minimally in Győr. In Debrecen the station relocation caused no significant changes in basic wind statistics as earlier studies showed (*Tar* and *Kircsi*, 2001), unlike Győr, where significant changes can be shown by a simple homogeneity test of the wind data. The reason for this is probably the different environment of the new location. Hence, only the data of those stations are applied, where monthly data series can be regarded homogeneous from January 1991 to December 2001. Thus, anemometric conditions can be considered constant in the following stations: Debrecen, Szeged, Budapest, Pécs, Keszthely, Szombathely, and Kékestető. *Table 1* shows the exact geographical coordinates of the observatories and the height of the wind-gauge above the ground level. We will distinguish lowland (Debrecen, Szeged and Budapest), non-lowland (Pécs, Keszthely, and Szombathely), and mountainous (Kékestető) stations.

Fig. 1. Geographical locations of the meteorological observatories comprising the whole database.

Table 1. Geographical coordinates (φ: latitude, λ: longitude, h: elevation) of the observatories comprising the processed database, and anemometer altitudes (h_a)

Observatory	φ	λ	**h (m)**	**h_a (m)**
			1991–2000	
Kékestető	47°52'	20°01'	1011	26
non-lowland				
Szombathely	47°16'	16°38'	219	9
Keszthely	46°46'	17°14'	117	15
Pécs	46°00'	18°14'	201	10
lowland				
Budapest-Lőrinc	47°27'	19°13'	130	12
Szeged	46°15'	20°06'	83	9
Debrecen	47°30'	21°38'	111	10

3. *Determining monthly average specific wind power with an approximation function*

Properties of the monthly average specific wind power can be described with the definite integral (area under the curve) of proportional trigonometric polynomial matching the hourly averages of the cubes of wind velocities. An index number for the approximation of the above function is defined, and its spatial variation is analyzed. The conclusions concerning the daily course of wind energy are drawn from the discussion of the suddenness and its relation with the weather situation in the daily and 12-hour waves of the approximation function.

3.1. The method

Wind velocities at discrete measurement times for each day of a specific period are given. The dependence on the number of measurement times is eliminated if a continuous approximation function is found, and the area under its curve can be determined by analytic integration.

Specific wind power falling on a day of a period of time on average is defined as half of the air density multiplied by the area under a function curve that approximates the daily course of the averages of wind speed cubes by measurement time.

The approximation function is

$$f_2(x) = a_0 + \sum_{m=1}^{2}(a_m \cos\frac{2\pi mx}{N} + b_m \sin\frac{2\pi mx}{N}). \tag{2}$$

It contains the first two members of a Fourier series consisting of trigonometric polynomials, where N is the number of daily measurement times, and $x = 0, 1, 2, ..., N-1$. The so-called residual variance describes the correctness of the approximation or fitting:

$$s_m^2 = s_{m-1}^2 - 0.5A_m^2, \tag{3}$$

where $s_0^2 = s_n^2$, thus, the square of the deviation is

$$A_m = (a_m^2 + b_m^2)^{1/2}, \tag{4}$$

which is the amplitude of the wave m (*Dobosi* and *Felméry*, 1971). It is obvious, though, that s_m^2 depends on the size of the data, and thus, it is not applicable for comparison in this case. For that purpose, the parameter determining the relative amount of approximation is used:

$$s_{0m} = \frac{s_0^2 - s_m^2}{s_0^2}, \tag{5}$$

which might be considered as independent value, thus, it depends not on the magnitude of wind velocities, and it needs not to be corrected for anemometer altitude. s_m^2 values are obviously reduced as the number of approximating polynomials is increased. Let us assume the opposite, when $s_m^2 \approx s_0^2$, that is $s_{0m} \approx 0$. If, however, approximation with Eq. (2) is "perfect", then $s_m^2 \approx 0$, that is $s_{0m} \approx 1$. The closer the s_{0m} falls to 1, the better the approximation function fits the average (*Tar* and *Kircsi*, 2001; *Tar et al.*, 2002).

The primitive of Eq. (2) is

$$F_2(x) = a_0 x + \sum_{m=1}^{2} \left(\frac{a_m}{\alpha_m} \sin \alpha_m x - \frac{b_m}{\alpha_m} \cos \alpha_m x \right), \tag{6}$$

where $\alpha_m = {}^{2\pi m}/_{N}$. Consequently, if we use the time series of the averages of wind speed cubes by measurement times to determine coefficients a_m and b_m, the average specific wind power falling on a day in the period (P_{fmd}) is

$$P_{fmd} = \frac{\rho}{2} [F_2(N-1) - F_2(0)],$$

where

$$T_{ga} = F_2(N-1) - F_2(0) \tag{7}$$

is the area under the curve. The definite integral gives the area under the curve in units determined by the values of x, which depends on the number of measurement times chosen to specify in a day. This fact must be taken into consideration when comparing calculated values.

In the following sections the time series of average wind power falling on a day of a month is described, i.e., the method described above is applied for all the months in the period between 1991 and 2000 at all of the seven stations.

3.2. Fit of the approximation function

First the spatial variation of the dimension defined by Eq. (5) is analyzed. *Table 2* contains the most important statistical properties of this parameter. The averages show that the approximation was the best in Szeged and Debrecen, while it was the worst in Keszthely and Pécs. The variability of the parameter, which is indicated by the range, i.e., the difference between the extremities, or by the variation coefficient, appears in the reverse sequence of the previous series in general. Maximum values mainly occur in the spring and summer months, but

never in autumn or winter, while the minimum values appear only in winter. The correlation coefficients between s_{02} and the mean monthly wind velocity [v] are also calculated, as it is might be assumed that the goodness-of-fit depends on this velocity. The respective threshold values for significance levels of 0.05 and 0.10 are $|r_{0.05}| \approx 0.1793$, and $|r_{0.10}| \approx 0.1509$ assuming the element number to be $n \approx 120$. The next to the last row in the table shows that stochastic relationship exists everywhere at least on the 0.05 significance level, except for Kékestető.

Table 2. Essential statistical properties of the parameter s_{02} describing the goodness of approximation (v: monthly mean wind velocity)

	Debrecen	**Szeged**	**Budapest**	**Pécs**	**Keszthely**	**Szombathely**	**Kékestető**
Mean	0.77	0.79	0.74	0.68	0.71	0.76	0.76
St.deviation	0.17	0.15	0.18	0.21	0.21	0.17	0.16
Maximum	0.98	0.96	0.95	0.96	0.95	0.96	0.97
Minimum	0.13	0.30	0.10	0.07	0.03	0.13	0.13
Range	0.85	0.66	0.85	0.89	0.92	0.83	0.84
Correlation coefficient (s_{02}, v)	0.2042	0.2408	0.2198	0.2086	0.1863	0.2960	0.1326
> %	63.3	62.5	60.8	61.7	61.0	59.3	64.2

The last row of Table 2 lists the relative frequency in percentage of those parameter values s_{02} that exceed the average. It is the lowest at Szombathely and the highest at Kékestető, a frequency well beyond 50 percent.

There is no observable annual cycle in the appearance of elements exceeding the average due to the small number of cases. If, however, all seven stations are treated together, the values in March and April as well as those in September and October are beyond 10%, representing 43.7% in total. It is remarkable that minimums are found very close to 0 within the extreme values. The absolute minimum is 0.03 which occurred in December 2000 in Keszthely. The absolute maximum is 0.98 which occurred in August 1994 in Debrecen.

3.3. Suddenness of the approximation function

Fourier analysis calls the expected value of amplitudes expectancy (E):

$$E = s_n \sqrt{\frac{\pi}{N}} . \tag{8}$$

To decide whether the period N/m of the m wave is random or real, the relation between A_m amplitude and E expectancy is used. In the case when A_m / E is large enough, the probability (p) of random order in the data is low, thus, it can

be considered statistically real. In general, $A_m / E > 2$ is acceptable ($p = 0.05$), but in the periodic analysis of time series of meteorological data the wave is considered real, when $A_m / E > 1.5$ ($p = 0.17$) is met (*Koppány*, 1978).

Table 3 shows that the daily wave must not be considered random in 80 to 95% of the cases at the significance level of 0.05 and in 89.2 to 97.5% of the cases at the 0.17 significance level, as it was expected. More interesting is the suddenness of the 12-hour wave, where the ranges in the table are 11.7 to 25% and 29.2 to 57.5%, respectively.

Table 3. Percentages of the reality of the daily and 12-hour waves at significance levels of 0.05 ($A_m/E>2$) and 0.17 ($A_m/E > 1.5$)

%	Debrecen	Szeged	Budapest	Pécs	Keszthely	Szombathely	Kékestető
$A_1/E>2$	95.0	92.5	95.0	80.0	88.3	94.2	91.7
$A_1/E>1.5$	97.5	95.8	95.8	89.2	92.5	97.5	95.0
$A_2/E>2$	12.5	24.2	11.7	25.0	12.5	17.5	17.5
$A_2/E>1.5$	40.0	50.0	38.3	57.5	36.7	40.8	29.2

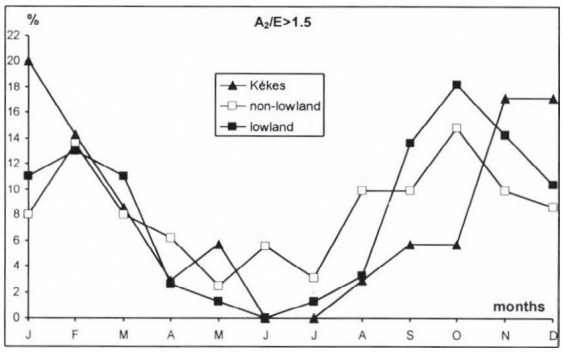

Fig. 2. Monthly frequencies of the reality of the 12-hour wave (p = 0.17).

According to the Introduction, let us take a closer look at the annual variation of the non-random 12-hour waves at the 0.17 significance level. We will examine the monthly distribution of those cases, where A_2 / E is greater than 1.5 according to station types. *Fig. 2* shows the frequency of fulfilled conditions in percentage for every station types. It is clear from the figure that the condition is not realized in June at the lowland stations where the frequency raises above 10% in the autumn and winter months as well as in March. The maximum is in October while the secondary maximum occurs in February. The months for the annual maximum and secondary maximum are the same in the

case of non-lowland stations, but the value of the primary maximum reduces in favor of June, when an approximately 6% high tertiary maximum occurs. In Kékestető the yearly course is simpler and smoother: there are two zero minimums in June and July, and a maximum of about 20% in January with large winter values.

We can see that the 12-hour wave of trigonometric polynomials fitted monthly on the average cubes of the hourly wind velocities shows suddenness mainly in the late spring and summer months at the 0.17 significance level, while the frequency of its probable reality increases in the winter, early spring, and autumn months, that is for the major part of the year. Thus, we may expect significant daily alterations of wind energy, its morning and afternoon minimums, as well as its daytime and night maximums (the other way round in the case of Kékestető). There is no circadian change of wind energy in those cases, where the 12-hour wave is random, for they are dominated by the daily cycle with a single maximum around midday. *Fig. 3* illustrates the above, where the hourly average of measured cubes of wind speeds appear by months corresponding to the absolute extreme A_2 / E ratios together with approximate values of waves 1 and 2. The column *b* of the figure clearly shows that at minimal A_2 / E ratio the two waves practically coincide, i.e., the approximation slightly increases including the second random wave.

Fig. 4 shows daily differences in the cases of extreme values in observatory types, they indicate the deviation of the hourly average wind speed cubes from the daily maximum in percentage based on the approximate data. As it follows from the part *a* of *Fig. 4*, if the 12-hour wave is real, there is no great difference between the values of lowland and non-lowland stations. Maximums fall approximately between 65 and 70% on both station types. The daily difference is the lowest in Kékestető, where it raises above 40% only in the early afternoon. According to part *b* of the figure, in the case of a non-dominant, random 12-hour wave, the greatest differences from the daily maximums in the night are over 70% in the average of lowland stations. In Kékestető the differences have a daily maximum over 65% around midday.

Assuming a 0.17 significance level, the frequency of advantageous days for electric energy production from wind is between approximately 43 and 70% in all the seven stations. Kékestető has the most of them with Keszthely, Budapest Debrecen, Szombathely, Szeged, and Pécs following in order. The cases when the daily wave dominates and is accompanied by random 12-hour waves, that is $A_1 / E > 1.5$ and $A_2 / E \leq 1.5$, have not yet been discussed. The number of these cases is expected to be relatively great. Their proportion (to the number of all months) by station types is 63.6% in lowland stations, 58.3% in non-lowland stations without Kékestető and 60.4% with it, while 61.8% in all of the seven stations together.

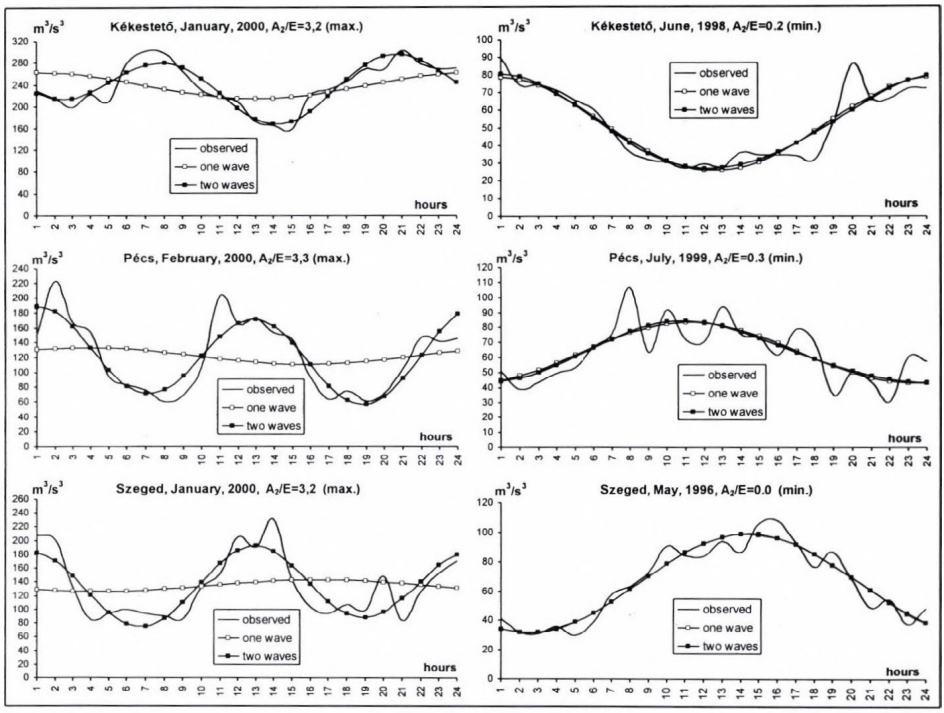

(a) (b)

Fig. 3. Examples for approximation with one and two waves of hourly averages of wind speed cubes (m^3/s^3) in the case of very strong (a) and very week (b) 12-hour periods.

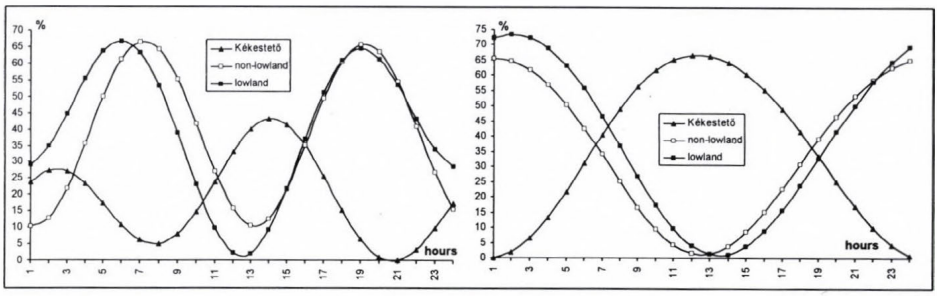

(a) (b)

Fig. 4. Deviation of the average of hourly wind speed cubes from daily maximums in the case of real (a) and random (b) 12-hour wave (from the extreme values of observatory types).

The most favorable days for the system administration are very likely those when there is no significant daily variation. Following from the above, the

number of such days must be relatively small. The number of months where the daily average wind power shows neither the daily nor the 12-hour cycle on the 0.17 significance level is altogether 17 days, which is only 2% in the period discussed here.

4. Relation of the daily course with the weather situations

Next, we attempt to analyze the interrelation between the reality of the 12-hour period with the weather situations in detail, and to analyze it shortly in the case of daily period. The daily flow conditions with the Péczely's macrosynoptic situations (*Péczely*, 1961, 1983) and with the Hess-Brezowsky macrocirculational types (*Hess* and *Brezowsky*, 1977) are described together with Puskás' weather front types (*Puskás* and *Nowinszky*, 1996; *Puskás*, 2001). Then types, dominate at the seven observation stations in those months, which meet the condition $A_2 / E > 1.5$, is determined.

4.1. Relation between the 12-hour and daily period and Péczely's macrosynoptic conditions

Table 4 summarizes the codes, letter codes, and short descriptions of Péczely's macrosynoptic types (*Péczely*, 1983). It is apparent that both meridional (MN, MS) and zonal (ZW, ZE) type-groups can be created, while central types cannot be grouped. It is also common to gather the types into cyclonic (CG: 1, 3, 4, 6, 7, 13) and anticyclonic (AG: 2, 5, 8, 9, 10, 11, 12) type-groups.

Next, we examine which types and type-groups are dominant in those months when the average daily course of wind energy has real 12-hour periodicity ($A_2 / E > 1.5$). Such dominance is measured with the occurrence of a given type or type-group in percent compared to the number of all occurrences in the month that fulfills the above condition. In Debrecen, for instance, the mCc type if the condition is met occurs on 171 days out of the 457 days within the whole period, thus, its relative frequency is $100 \cdot 171/457 = 34.4\%$.

Fig. 5 displays the frequency of each type in the decade from 1991 to 2000 (*Károssy*, 1993, 1998, 2001). The figure also shows that the days characterized by the zC (zonal–cyclonic) type in the months fulfilling the reality condition occur most frequently at the three station types. According to the figure, zC type is the second rarest condition in the period of our study, as well as in the period from 1971 to 2001 (2.2 and 3.1%, respectively). Its flow is typically directed from west to east, and for the most part it is characterized by windy and changeable weather. As the figure shows, average conditional frequencies do not significantly differ from each other at the lowland and non-lowland stations. On the other hand, the relative frequency at Kékestető rises above 40% only in the case of type zC. The rarest occurrence of the 12-hour period may be expected in

the case of AB, AF, and C types: below 40% at the lowland and non-lowland stations, bellow 25% at Kékestető.

Table 4. Codes, letter codes, and short descriptions of Péczely's macrosynoptic types

Meridional directed types with northern current (MN type-group)		
1	mCc	Hungary lies in the rear of an east-European cyclone
2	AB	anticyclone over the British Isles
3	CMc	Hungary lies in the rear of a Mediterranean cyclone
Meridional directed types with southern current (MS type-group)		
4	mCw	Hungary lies in the fore part of a west-European cyclone
5	Ae	anticyclone to the east of Hungary
6	CMw	Hungary lies in the fore part of a Mediterranean cyclone
Zonal directed types with western current (ZW type-group)		
7	zC	zonal cyclone type
8	Aw	anticyclone extending from the west
9	As	anticyclone in the south of Hungary
Zonal directed types with eastern current (ZE type-group)		
10	An	anticyclone in the north of Hungary
11	AF	anticyclone over the Fennoscandinavian region
Central types		
12	A	anticyclone over the Carpathian Basin
13	C	cyclone over the Carpathian Basin

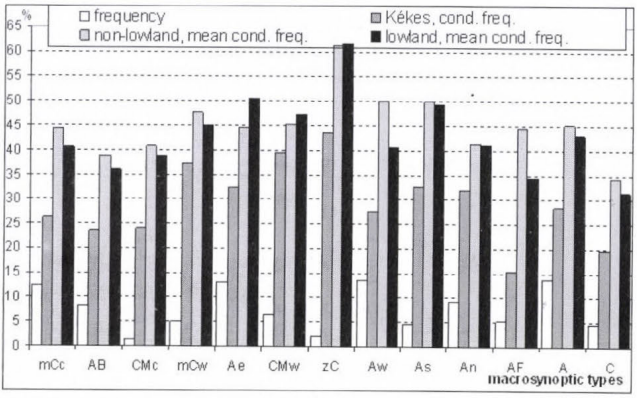

Fig. 5. Frequencies of Péczely's macrosynoptic types in percent of the total number of days of the period studied, and their conditional ($A_2/E>1.5$) frequency in the presence of real 12-hour periods.

Table 5 shows the frequency of individual macrosynoptic type-groups and their conditional frequency in the presence of 12-hour periods. It is clear that anticyclonic conditions (AG) occur twice as frequently as cyclonic ones, as well as there is a more than 10 percent dominance of meridional (MN + MS)

conditions. According to the table, MS types occur most frequently at lowland stations, while types belonging to the ZW group occur most frequently at non-lowland locations, if there is a real 12-hour periodicity. However, the absolute maximum is found at the ZE type-group in Debrecen. According to the same table, cyclonic (CG) and anticyclonic type-groups do not differ significantly in this respect; the greatest difference in their frequency (6.2%) was observable in Pécs.

Table 5. Frequency of individual Péczely's macrosynoptic type-groups and their conditional ($A_2/E>1.5$) frequency in the presence of real 12-hour periods

$A_2/E>1.5$	MN	MS	ZW	ZE	CG	AG
Frequency (%)	22.4	24.6	20.4	14.4	32.3	67.7
			Conditional frequency (%)			
Debrecen	62.9	52.9	56.0	65.7	58.5	59.5
Szeged	42.8	57.0	52.2	47.6	48.5	50.2
Budapest	36.6	43.3	39.4	34.9	39.0	38.0
Pécs	54.2	55.5	62.8	60.6	53.3	59.5
Keszthely	34.4	36.6	43.8	29.3	36.0	36.5
Szombathely	37.5	43.9	46.8	37.5	44.4	38.8
Kékes	25.1	35.3	30.5	26.1	30.8	28.2
Mean	41.9	46.4	47.4	43.1	44.4	44.4

As we can see in *Table 3*, the frequency of real daily wave is a long sight larger than the frequency of the 12-hour period. It is located between 80 and 95% on the 0.05 significance level. So we can calculate with a great safety on the appearance of twenty four-hour period in all day. It follows from this, that the conditional frequencies of these do not differ from each other in the various macrosynoptic types and type-groups. For example, we find the next in the different type-groups: the maximum conditional frequency is in the type-group MN in the case of six observatories, the minimum conditional frequency is in the type-group MS in five observatories, there is no maximum or minimum value in the MS and ZW, or MN and ZE type-groups. So the extreme values are in the meridional groups. If only the cyclonic and anticyclonic groups are distinguished (see *Table 5*), we can find that the conditional frequencies are not differ each other significantly on the stations, namely the reality of the whole day wave is independent of these groups.

4.2. Relation between the 12-hour and daily period and the Hess–Brezowsky macro-circulational types

The classification of Hess–Brezowsky macrosynaptic weather types was made with regards to the circulation conditions of the Atlantic-European region and

the directions of major frontal zones (*Hess* and *Brezowsky*, 1977). Altogether 29 types (4 zonal, 7 mixed, and 18 meridional) are distinguished and an additional type is defined for the untypical fields. *Table 6* lists the types and groups that can be formed from them according to *Bárdossy* and *Caspary* (1990) and *Bartholy* (2005). We use the daily codes for the period in question from the work of *Gerstengarbe* and *Werner* (2006).

Due to the small size of our database, only the 10 groups distinguished by the main flow direction and three circulation types (zonal, mixed, meridional) were investigated. For easier identification the letters of the circulation types were appended to the beginning of the letter codes of the 10 groups in *Table 6.*

Table 6. List of Hess-Brezowsky major types (GWT)

Major type/groups (GWT)	Main direction of the flow
A. zonal circulation (z)	
West	zW
B. mixed circulation (x)	
Central European high	xHM
Central European low	xTM
Southwest	xSW
Northwest	xNW
C. meridional circulation (m)	
East	mE
South	mS
Southeast	mSE
North	mN
Northeast	mNE

In the next step, type-groups dominating in those months when the average daily course of the wind energy shows real 12-hour periodicity ($A_2 / E > 1.5$) were examined. *Fig. 6* displays the frequency and conditional frequency of each type-group. According to the figure, there are not so much apparent orders as in the case of Péczely's types. The figure leads us to the following conclusion: we can least (somewhat more than 30%) expect the occurrence of the real 12-hour period in the merdional type-group with northeastern main flow direction (indicated as mNE in the figure), while the period will occur most frequently (approximately 50%) in the also meridional, mSE type at the lowland stations.

The absolute maximum occur at the non-lowland stations with the mixed cyclonic type-group (xTM) – almost 2/3 of such days have real 12-hour periods. It is flowed by the zonal west group (zW), where the proportion of real periods is 52%. The absolute minimum (12.5%) is in Kékestető with the meridional NE main flow directional type-group (see above). It is followed by xTM, which is the absolute maximum and the maximum at the non-lowland stations.

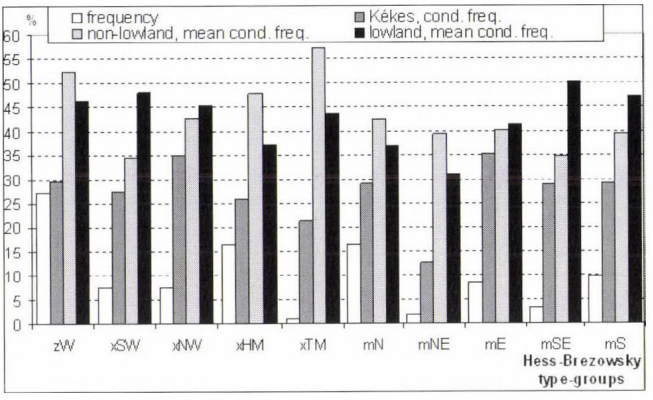

Fig. 6. Frequency of various Hess-Brezowsky macrosynoptic type-groups in per cent of the total number of days of the period studied and their conditional frequency in the presence of real 12-hour periods.

Table 7 contains the frequencies and conditional frequencies of the zonal group and that of the combined mixed and meridional groups. The dominance of the meridional type-group and the northern direction within it is obvious, while it is the anticyclonic group those duffers in the mixed type. The maximum relative frequency falls to Pécs, the minimal one is in Kékestető in all three groups. According to the averages of all stations, the real 12-hour period occurs most frequently in the zonal, while less frequently in the meridional type-group.

The investigation at the 0.05 significance level of reality of daily period shows, that the conditional frequencies reach 100% in the xTM circulation type in four observatories (three lowland stations and Kékestető) and in the mNE type in Debrecen. Investigation by type-groups we find that the maximum or its approximate values are in the mixed (x) group, and the minimum values are in the zonal (z) group.

Table 7. Frequency of various Hess-Brezowsky circulation type-groups and their conditional frequency in the presence of real twelve-hour periods

A_2/E>1.5	Zonal	Mixed	Meridional
Frequency (%)	27.4	32.3	40.3
Conditional frequency (%)			
Debrecen	44.7	36.6	39.3
Szeged	54.7	48.7	46.9
Budapest	39.0	39.8	36.9
Pécs	64.7	58.3	51.8
Keszthely	45.6	33.8	32.2
Szombathely	46.6	39.7	37.4
Kékes	29.6	28.2	29.6
Mean	46.4	40.7	39.2

4.3. Relation between the 12-hour and daily period and the weather front types

It is well known that frontal passages are accompanied by more or less marked changes in the weather that might be analyzed in details if the weather fronts are classified into different types and the weather characteristics of individual front types are discerned.

The classification of weather fronts may be based on various aspects. *Berkes* (1961) gave 22 front types for the area of Hungary based on detailed air mass analysis by the help of radio probe launches. The front almanac of the Hungarian Meteorological Service uses the same front types. Another, more accurate method of front analysis, which requires a very large database, is the examination of geopotential fields (*Bartholy et al.*, 2006).

Front types based on complicated definitions are rather cumbersome to use in practice, therefore, a simpler front definition method that requires only basic meteorological expertise became necessary. *Puskás* and *Nowinszky* (1996) and *Puskás* (2001) have carried out the classification of fronts passing over Hungary by the help of the synoptic maps for the "Daily Meterorological Reports" of the Hungarian Meteoroligal Service as well as the recorded weather measurement data. *Fig. 7* lists the 9 front types (t1–t9) they have distinguished.

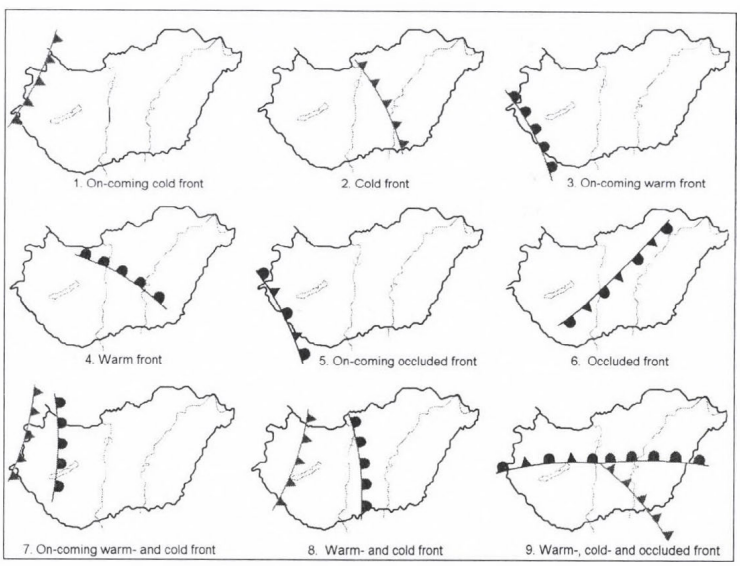

Fig. 7. Weather front types (t1–t9) in Hungary.

Fig. 8 shows the frequency of front types in percent of days with frontal passage. It clearly shows that the most frequent front type is the on-coming cold front (t1) and the rarest type is the simultaneous stationary cold, warm, and occluded front (t9). Cold front types (t1 and t2) occur altogether in 42.3%, warm

fronts (t3 and t4) in 28.4%, and both fronts (t7 and t8, without occlusion) in 18.3%, while occluded fronts (t8, t6 and t9) occur in the 10.9% of the cases.

We have examined which front types are dominant in those months when the course of the average daily wind energy shows real 12-hour periodicity. *Fig. 8* also displays the conditional frequency of each type if the condition $A_2 / E \geq 1.5$ is met. This figure allows for some general conclusions to be drawn: there is always warm front (t3 or t7) present at each observation types when local maximums occur. Minimums are always observed in the presence of one of the occluded front types (t5, t6 or t9). The figure shows that real 12-hour periodicity on the whole scale occurs most frequently in the case of two warm front types (t3 and t4). The next probable cases are the approaching warm and cold fronts (t7), while it occurs least frequently in the case of the two occluded front types.

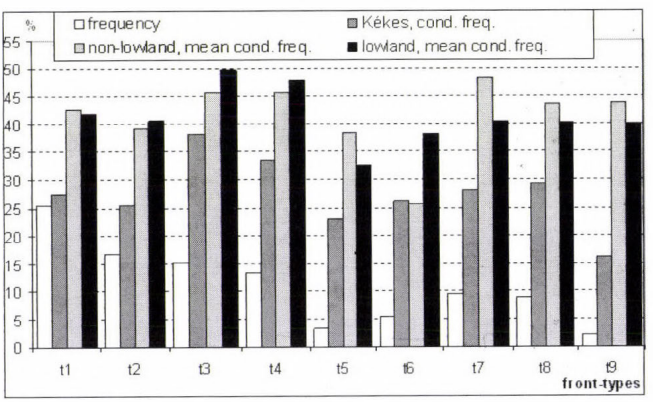

Fig. 8. Frequency of individual front types in percent of the number of days with frontal passage and their conditional frequency in the presence of real 12-hour periods.

If we consider only the days with and without frontal passage (cf. *Table 8*), we may see that the number of days without fronts in the period of our study is more than double of the number of days with frontal passage.

Their conditional frequencies by observation stations and on the average hardly differ, the presence of real 12-hour periodicity is given. Except for Keszthely, this frequency for days with frontal passage is always higher by some tenth % and we find the maximal 3% difference in Szombathely.

The investigation at the 0.05 significance level of reality of daily period shows that the conditional frequencies reach 100% in the t9 type at Debrecen and Kékestető. On the other hand, the maximum values distribute evenly in types t1, t2, t4, t7, t8, and t9, namely they do not occur in types t3, t5, and t6. However, the minimum values are concentrated in t3 type, so the probability of the reality of the daily period is the least in this type. If only the days with and

without fronts are distinguished, then the conditional probabilities do not differ each other significantly, namely the reality of the whole day wave is independent of such days.

Table 8. Frequency of days without and with frontal passage in percent of the total number of days of the period studied, and the conditional frequency of days with and without frontal passage in the presence of real 12-hour periods

$A_2/E>1.5$	Without fronts	With fronts
Frequency (%)	68.7	31.3
	Conditional frequency (%)	
Debrecen	39.8	40.2
Szeged	49.6	49.7
Budapest	38.1	38.7
Pécs	57.3	58.0
Keszthely	36.4	36.3
Szombathely	30.4	33.4
Kékes	28.9	29.3
Mean	40.1	40.8

5. Conclusions

It can be shown by the aid of fitting trigonometric polynomials that the hourly average of wind speed cubes – i.e., the hourly average specific wind power – follows one of three possible daily patterns. Single daily maximal and minimal value occur in the first case, while two daily maxima and minima appear in the second one. In the third case, there is no actual daily pattern, but the hourly values show random fluctuation. Seasonal distribution of the above cases may provide useful information for energetic systems management, when wind power is used to produce electricity:

- The 12-hour period mostly shows randomness in late spring and summer months, the reality of the first (24-hour) wave increases with the randomness of the second one in these months. Thus, we may rather safely assume that diurnal changes of wind energy will follow patterns that are favorable for energetic systems management in spring and summer. The number of most favorable days for the systems management, where there is no significant daily course at all, is few. The frequency of those months when average daily wind power shows neither diurnal nor 12-hour cycles, is only 2% in the period examined.
- In the majority of the observation stations, days that can be characterized as zC (zonal cyclonic) types according to Péczely's classification are the most frequent in those months, where the hourly

average wind power has real 12-hour period. Its flow is typical west to east, characterized mostly by steady wind and changeable weather. We may least expect the occurrence of 12-hour periods in the case of the AB, AF, and C types.

- 12-hour periods occur least frequently in the meridional northeast main flow direction type-group, while they will occur most frequently in zonal west and mixed cyclic type-groups in the case of Hess-Brezowsky classification.
- If we separate the days with or without frontal passage, we find that their frequency by observation stations and on the average hardly differs, the presence of real 12-hour periodicity is proven. Considering the front types, maximum always occurs in the presence of warm front at each stations, while minimum mostly occurs together with an occluded front type. Averages show that real 12-hour periodicity occurs most frequently with warm front types, together with approaching warm and cold fronts, but least frequently with the two occluded front types.

Acknowledgements—The author expresses his gratitude to the Hungarian Meteorological Service for providing the wind data necessary for his research.

References

Bárdossy, A. and *Caspary, H.J.*, 1990: Detection of climate change in Europe by analyzing European atmospheric circulation patterns from 1881 to 1989. *Theor. Appl. Climatol. 42*, 155–1671.

Bartholy, J., 2005: Reconstruction of climatic past of Carpathian Basin and the estimate of the expected tendencies in the future (in Hungarian). *DSc Thesis*, Magyar Tudományos Akadémia, Budapest, Hungary.

Bartholy, J., Pongrácz, R., and *Pattantyús-Ábrahám, M.*, 2006: European cyclone track analysis based on ECMWF ERA-40 datasets. *Int. J. Climatol. 26*, 1517-1527.

Berkes, Z., 1961: Air-masses and front types in the Carpathian Basin (in Hungarian). *Időjárás* 65, 289-293.

Dobosi, Z. and *Felméry, L.*, 1971: *Climatology* (in Hungarian). Tankönyvkiadó, Budapest.

Gerstengarbe, F.-W. and *Werner, P.C.*, 2006: Katalog der Grosswetterlagen Europas (1881-2004). *PIK Report* No. 100. http://www.pik-potsdam.de/publications/pik_reports/reports/pr.100/pr100.pdf

Hess, P. and *Brezowsky, H.*, 1977: *Katalog der Grosswetterlagen Europas*. Berichte des Deutschen Wetterdienst, 113, 15.

Károssy, Cs., 1993: Péczely's classification of macro-synoptic types and catalogue of weather situations (1951-1992). In *Light Trapping of Insects Influenced by Abiotic Factors.* Part I. (ed.: *L. Nowinszky*). Publisher OSKAR, Szombathely, 113-126.

Károssy, Cs., 1998: Péczely's classification of macro-synoptic types and catalogue of weather situations (1992-1997). In *Light Trapping of Insects Influenced by Abiotic Factors.* Part II. (ed.: *L. Nowinszky*). Savaria University Press, Szombathely, 117-130.

Károssy, Cs., 2001: Characterisation and catalogue of the Péczely's macrosynoptic weather types (1996-2000). In *Light Trapping of Insects Influenced by Abiotic Factors.* Part III. (ed.: *L. Nowinszky*). Savaria University Press, Szombathely, 75-86.

Koppány, Gy., 1978: *Long-Range Forecast* (in Hungarian). Tankönyvkiadó, Budapest.

Péczely, Gy., 1961: *Climatic characterization of macro-synoptic types in Hungary* (in Hungarian). Országos Meteorológiai Szolgálat Kisebb Kiadványai 32, Budapest.

Péczely, Gy., 1983: *Catalogue of the macrosynoptic types for Hungary (1881-1983)* (in Hungarian). Országos Meteorológiai Szolgálat Kisebb Kiadványai, 53, Budapest.

Puskás, J., 2001: New weather front types and catalogue for the Carpathian Basin. In *Light Trapping of Insects Influenced by Abiotic Factors.* Part III. (ed.: *L. Nowinszky*). Savaria University Press, Szombathely, 87-118.

Puskás, J. and *Nowinszky, L.*, 1996: Light-trap catch of the turnip moth (Scotia segetum Schiff.) during the time of weather fronts (in Hungarian). *Légkör* XLI., No. 2, 29-32.

Stróbl, A., 2006: Extra load of wind turbines in our electric energy system (in Hungarian). *Magyar Energetika 4*, 33-43.

Tar, K. and *Kircsi, A.*, 2001: A method for calculation of the daily specific wind power (in Hungarian). In *Meteorological Scientific Days — Meteorological Basics of the Atmospheric Resources Utilization* (ed.: *J. Mika*). Országos Meteorológiai Szolgálat, Budapest, 129-137.

Tar, K., Kircsi, A., and *Vágvölgyi, S.*, 2002: Temporal changes of wind energy in connection with the climatic change. In *Proc. of the Global Windpower Conference and Exhibition.* CD-ROM, Paris.

IDŐJÁRÁS

VOLUME 111 * 2007

BUDAPEST, HUNGARY

AUTHOR INDEX

TABLE OF CONTENTS
Papers

SUBJECT INDEX

T

U

V

W

GUIDE FOR AUTHORS OF *IDŐJÁRÁS*

The purpose of the journal is to publish papers in any field of meteorology and atmosphere related scientific areas. These may be

- research papers on new results of scientific investigations,
- critical review articles summarizing the current state of art of a certain topic,
- short contributions dealing with a particular question.

Some issues contain "News" and "Book review", therefore, such contributions are also welcome. The papers must be in American English and should be checked by a native speaker if necessary.

Authors are requested to send their manuscripts to

Editor-in Chief of IDŐJÁRÁS

P.O. Box 39, H-1675 Budapest, Hungary

in three identical printed copies including all illustrations. Papers will then be reviewed normally by two independent referees, who remain unidentified for the author(s). The Editor-in-Chief will inform the author(s) whether or not the paper is acceptable for publication, and what modifications, if any, are necessary.

Please, follow the order given below when typing manuscripts.

Title part: should consist of the title, the name(s) of the author(s), their affiliation(s) including full postal and e-mail address(es). In case of more than one author, the corresponding author must be identified.

Abstract: should contain the purpose, the applied data and methods as well as the basic conclusion(s) of the paper.

Key-words: must be included (from 5 to 10) to help to classify the topic.

Text: has to be typed in single spacing with wide margins on one side of an A4 size white paper. Use of S.I. units are expected, and the use of negative exponent is preferred to fractional sign. Mathematical formulae are expected to be as simple as possible and numbered in parentheses at the right margin.

All publications cited in the text should be presented in a *list of references*, arranged in alphabetical order. For an article: name(s) of author(s) in Italics, year, title of article, name of journal, volume, number (the latter two in Italics) and pages. E.g., *Nathan, K.K.,* 1986: A note on the relationship between photo-synthetically active radiation and cloud amount. *Időjárás 90,* 10-13. For a book: name(s) of author(s), year, title of the book (all in Italics except the year), publisher and place of publication. E.g., *Junge, C.E.,* 1963: *Air Chemistry and Radioactivity.* Academic Press, New York and London. Reference in the text should contain the name(s) of the author(s) in Italics and year of publication. E.g., in the case of one author: *Miller* (1989); in the case of two authors: *Gamov* and *Cleveland* (1973); and if there are more than two authors: *Smith et al.* (1990). If the name of the author cannot be fitted into the text: *(Miller,* 1989); etc. When referring papers published in the same year by the same author, letters a, b, c, etc. should follow the year of publication.

Tables should be marked by Arabic numbers and printed in separate sheets with their numbers and legends given below them. Avoid too lengthy or complicated tables, or tables duplicating results given in other form in the manuscript (e.g., graphs)

Figures should also be marked with Arabic numbers and printed in black and white in camera-ready form in separate sheets with their numbers and captions given below them. JPG, GIF, or XLS formats should be used for electronic artwork submission.

The text should be submitted both in manuscript and in electronic form, the latter on disks or in e-mail. Use standard 3.5" MS-DOS formatted diskette or CD for this purpose. MS Word format is preferred.

Reprints: authors receive 30 reprints free of charge. Additional reprints may be ordered at the authors' expense when sending back the proofs to the Editorial Office.

Information on the last issues: http://www.met.hu/Journal-Idojaras.php

Published by the Hungarian Meteorological Service

Budapest, Hungary

INDEX: 26 361

HU ISSN 0324-6329